MCAT Institute
Final Report
94-07

NASA-CR-196836

Shock-Tunnel Combustor Testing For Hypersonic Vehicles

Mark Loomis

July 1994

NCC2-738

MCAT Institute
3933 Blue Gum Drive
San Jose, CA 95127

(NASA-CR-196836) SHOCK-TUNNEL COMBUSTOR TESTING FOR HYPERSONIC VEHICLES Final Report (MCAT Inst.) 33 p

N95-11938

Unclas

G3/09 0022675

Hypersonic Propulsion Research in the NASA-Ames 16-Inch Shock Tunnel

Final Report For Co-Operative Agreement NCC2-738

Dr. Mark P. Loomis

Proposed configurations for the next generation of transatmospheric vehicles will rely on air breathing propulsion systems during all or part of their mission. At flight Mach numbers greater than about 7 these engines will operate in the supersonic combustion ramjet mode (scramjet). The design system used to develop these engines will involve the use of both computational and experimental tools. Key ground based engine performance data is required to provide calibration of the CFD tools used in the design system and also to provide engineering correlations in areas where computational tools are not sufficient to properly model the flow physics.

Ground testing of these engine concepts above Mach 8 requires high pressure, high enthalpy facilities such as shock tunnels and expansion tubes. These impulse, or short duration facilities have test times on the order of a millisecond, requiring high speed instrumentation and data systems. One such facility ideally suited for scramjet testing is the NASA-Ames 16-Inch shock tunnel, which over the last two years has completed a series of tests for the NASP (National Aero-Space Plane) program at simulated flight Mach numbers ranging from 12-16. The focus of this grant was to provide support on this activity for Dr. Mark Loomis, who served as chief test engineer.

The experimental programs consisted of a series of classified tests involving a near-full scale hydrogen fueled scramjet combustor model in the semi-free jet method of engine testing whereby the compressed forebody flow ahead of the cowl inlet is reproduced (see appendix A). The AIMHYE-1 (Ames Integrated Modular Hypersonic Engine) test entry for the NASP program was completed in April 1993, while AIMHYE-2 was completed in May 1994. The test entries were regarded as successful, resulting in some of the first data of its kind on the performance of a near full scale scramjet engine at Mach 12-16. The data was distributed to NASP team members for use in design system verification and development.

Due to the classified nature of the hardware and data, the data reports resulting from this work are classified and have been published as part of the NASP literature. However, an unclassified AIAA paper resulted from the work and has been included as appendix A which contains an overview of the test program and a description of some of the important issues.

The research was conducted in conjunction with the Aerothermodynamics branch under the supervision of Dr. G.S. Deiwert, the technical monitor and Dr. John Cavalowsky, the technical leader.

APPENDIX - A

AIAA-94-2519

Large Scale Scramjet Testing in the Ames 16-Inch Shock Tunnel

Mark Loomis
MCAT Institute
Moffett Field
California

AIAA 94-2519
Large Scale Scramjet Testing in the Ames 16-Inch Shock Tunnel

G. S. Deiwert and J. A. Cavolowsky
NASA Ames Research Center
Moffett Field, CA

M. P. Loomis
MCAT Institute
Moffett Field, CA

18th AIAA Aerospace Ground Testing Conference

June 20-23, 1994 / Colorado Springs, CO

Large Scale Scramjet Testing in the Ames 16-Inch Shock Tunnel

George S. Deiwert* and John A. Cavolowsky**
NASA Ames Research Center, Moffett Field, CA
and
Mark P. Loomis***
MCAT Institute, Moffett Field, CA

Abstract

Test techniques and strategies for large scale scramjet testing in large reflected shock tunnels are described. Semi-free jet combustor testing in the Ames 16-Inch combustion-driven shock tunnel is reported with generic data indicating flight simulation capability, test time, and combustor performance over the Mach 12 to 16 flight regime. Measurements necessary to assess combustor performance are identified and discussed. Facility limitations, and potential upgrades to relax these limitations, are identified.

Introduction

Hypersonic flight utilizing air breathing propulsion requires the development of supersonic combustion ramjet (scramjet) technology. The flow path and thrust performance of a scramjet is characterized by chemical as well as aerodynamic time scales. Scramjet propulsion differs substantially from lower speed concepts in that the propulsion flow path is highly integrated with the vehicle external aerodynamics. The flow is compressed under the vehicle forebody from the nose of the aircraft and through the inlet to the combustor, and expanded through the one-sided nozzle to provide the overall propulsion performance. In the combustor itself hydrogen fuel is injected supersonically into a shock dominated supersonic air stream where it mixes and burns. The mixing time scale and the combustion time scale are important in defining the overall performance of the engine. Supersonic mixing and combustion in the combustor begin when the free stream Mach number surpasses 6, and scramjet technology development, including ground test and real-gas CFD, begins at that point and extends to flight Mach numbers approaching orbital speeds of Mach 25.

Due to the combination of both chemical and aerodynamic time scales and the highly integrated propulsion flow path, ground test and analysis should, if possible, include large-to-full scale test articles at simulated flight conditions in a free-jet configuration. Such a ground test capability, however, is beyond our current means, and reliance on sub-scale and component testing must be complimented with real gas CFD analysis and, where possible, on flight data.

The purpose of this paper is to describe one method developed for flow path testing of large-to-full scale integrated (inlet/combustor/nozzle) components for flight Mach numbers greater than 8. The ground test facility and test technique will be illustrated and its

---

*Senior Staff Scientist, Associate Fellow AIAA.
**Research Scientist, Senior Member AIAA.
***Research Scientist, Member AIAA. Presently with Sterling Software, Inc., Palo Alto, CA

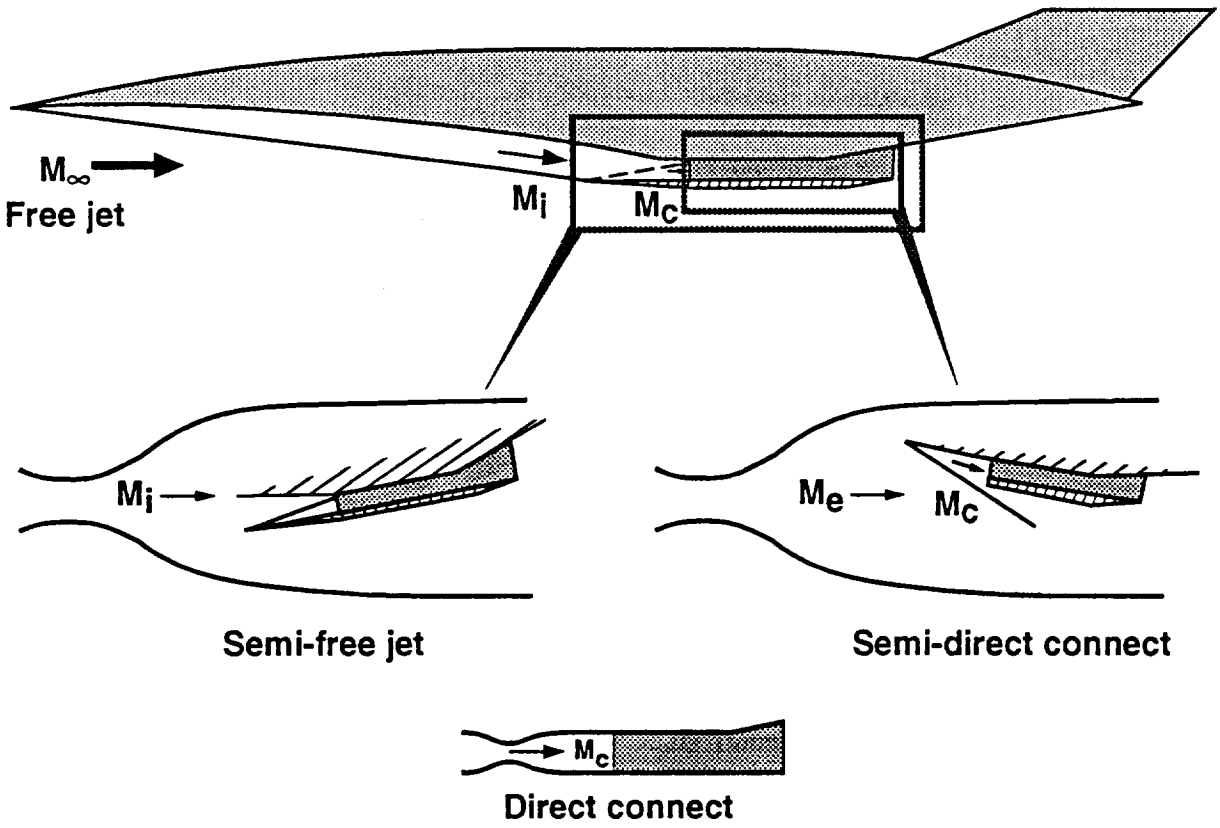

Fig. 1. Integrated scramjet ground test simulation configurations

value demonstrated using examples from recent and ongoing scramjet test programs conducted in the NASA Ames 16-Inch Combustion Driven Shock Tunnel.

As described by Billig et al[1] there are four basic techniques for configuring scramjet combustor tests. Illustrated in figure 1, these include (1) the free-jet configuration whereby the free stream and flow over the entire vehicle forebody is reproduced, (2) the semi-free jet configuration whereby the compressed forebody flow just ahead of the cowl inlet is produced, (3) the semi-direct-connect configuration and (4) the direct-connect configuration in which a one-dimensional flow is produced at the combustor entrance. In the free-jet configuration the entire forebody and combustor flow path would be replicated. As mentioned previously, current ground test capability does not yet exist to test in this configuration at or near full scale. In the semi-free jet configuration the flow behind the leading edge body shock is replicated by the flow from the ground test facility nozzle. Not simulated in this test configuration are leading edge bluntness effects, boundary layer transition and thickness, and shock-on-cowl interaction. Included, however, is the influence of the cowl and cowl shock, and a thin body-side boundary layer. A segment of a one-sided nozzle may be included at the end of the combustor. Hence, it is possible to account for two-dimensional inflow effects, including the important influence of the cowl shock, on combustor and nozzle performance. A facility large enough to accommodate test articles of large scale is required.

In the semi-direct-connect configuration, the cowl is eliminated and an over expanded flow from the test facility nozzle is turned through an oblique shock to produce one-dimensional flow conditions at the combustor entrance. A segment of the one-sided nozzle may be included at the

combustor exit. This technique may be used to trade excess facility total pressure for larger test article scale in smaller, high pressure facilities, by over expanding the flow to a large test section and recompressing to desired combustor entrance conditions.

The direct connect configuration also neglects the cowl; it provides one-dimensional flow conditions at the combustor entrance directly from the facility nozzle. Here the facility must be large enough to provide the mass flow rate for the combustor and need only have enough total pressure to provide the proper combustor inlet properties.

Large scale, long duration test facilities (vitiated blow down and arc heated facilities with test times in the order of several seconds or minutes) can provide enthalpy simulation for flight Mach numbers up to 13 for sub-scale integrated components in direct and semi-direct connect configurations. These facilities have some inherent test gas contamination due to the gas heating techniques used. For higher flight Mach numbers impulse facilities (such as shock tunnels and expansion tunnels) are required with test time in the order of milliseconds. These can provide good simulation up to Mach 14 and higher (up to Mach 17) with some test gas contamination by NO and O. The NASA facilities suitable for scramjet propulsion testing are summarized in Table 1. The Hypulse facility, an expansion tube located at GASL, is currently capable of providing flow path test simulation at Mach numbers of 14 and 17 for small combustor components in direct connect mode. The Ames 16-Inch combustion driven shock tunnel is currently capable of providing flow path test simulation at Mach numbers from 10 to 17 for large-to-full scale integrated combustors in semi-free jet mode. Two other facilities offer long duration flow times for large sub-scale components. The 8-ft High Temperature Tunnel at Langley can provide simulations at Mach numbers of 4, 5, 6.2 and 6.8 in semi-direct connect configuration, and the Ames DCAF (Direct Connect Arcjet Facility) can provide simulations at Mach numbers from 8 to 13 in direct connect mode.

Impulse Facilities

Facility	Test Time ms	Slug Length m	Core Flow cm	Flight Mach #
Hypulse	0.3-0.4	1.5	5-7.5	14 & 17
16-Inch	5.-10.	25	70	10 to 17

Long Duration Facilities

Facility	Test Time min	Mass Flow lb/s	Cross Section ft	Flight Mach #
8' HTT	2	400	8' dia	4, 5, 7
DCAF	30	8 to 12	2" x 14"	8 to 13

Table 1. NASA's Hypersonic Propulsion Ground Test Capability

Test Configuration

Given the limitations for testing full flight scale articles at flight test conditions, we choose here to attempt to establish a ground test capability for full scale integrated components, the preferred configuration being the semi-free jet concept.

"Full scale" is defined here to mean full scale fuel injectors in a full throat height, full length combustor. This is required to provide good simulation of both mixing and combustion time scales simultaneously. This implies a combustor entrance height on the order of 15 cm and a width at least twice that to minimize undesirable three-dimensional effects. For such a "full scale" test article the corresponding lengths of the cowl, combustor, and nozzle component are each of the order of 1 m.

To assure proper inlet profiles and mass capture comparable to the full flight vehicle, the test article should capture a two-dimensional flow from the core of

the facility nozzle. One way to assure this is to design the inlet body surface minimizing spillage and cross flow effects. This can be accomplished by flaring the surface outward laterally, in a trapezoidal shape, such that Mach waves generated at the corners of the leading edge are not captured in the combustor inlet. The cowl could be configured in a similar manner or configured with parallel sides using side strakes to control spillage. In this case the cowl should be substantially wider than the combustor entrance so that the vortical corner flow generated by the side strakes can be spilled off to the outside of the test article and only two-dimensional core flow is captured. A photograph of the full scale test article is shown in figure 2. This model was designed and built by GASL specifically for testing in the Ames shock tunnel. A schematic of the model is shown in figure 3 installed in the facility in semi-free jet configuration. As illustrated in figures 1 through 3, the cowl is angled downwards toward the nozzle wall. Parallel side strakes, which have been removed in the photograph for clarity, have been selected here to provide maximum width for a given facility size. Such considerations lead to an inlet width of about 0.6 m. The body side leading edge is co-aligned with the center of the facility nozzle. For a ground test facility to supply a uniform core flow of 0.6 m, the nozzle exit diameter should be about 1 m.

In a semi-free jet configuration the facility nozzle must replicate the flow behind the body shock just ahead of the cowl inlet. Shown in figure 4, are expected inlet conditions for a flight dynamic pressure of 1000 psf. The cowl turning angle, δ, is used as a parameter. For a cowl turning angle of, say, 12 degrees, and a flight Mach number of 12 at an altitude of about 35 km., these conditions are typically $M_i = 5.6$, $T_i = 1170$ K, $V_i = 3.5$ m/s, $p_i = 2.3$ psi. At Mach 16 at an altitude of about 40 km they are typically $M_i = 7.1$, $T_i = 1220$ K, $V_i = 4.9$ m/s, $p_i = 1.5$ psi. this will produce expected[2] combustor inlet conditions of $M_C = 4.45$, $T_C = 1500$ K, $V_C = 3.35$ m/s, and $p_C = 8.9$ psi, and $M_C = 5.45$, $T_C = 2055$ K, $V_C = 4.66$ m/s, and $p_C = 8.0$ psi, respectively.

To produce the required combustor inflow conditions for a given flight condition the critical facility parameters are reservoir pressure and nozzle area ratio. These two parameters provide the first order control of static pressure, temperature and Mach number at the combustor entrance. A third parameter, namely cowl turning angle, may be used to provide fine tuning adjustment if it is not fixed by model design constraints. Shown in figure 5, for a cowl turning angle of 12 degrees, the reservoir pressures to produce Mach 12 and 16 combustor inflow conditions are 6600 psi and 48,000 psi, and the nozzle expansion ratios are 130 and 940 respectively for a flight dynamic pressure of 1000 psf. Keeping in mind the requirement for a 1 m nozzle exit diameter it can be seen that the limiting facility parameter for the lower Mach number regime is the nozzle area ratio. For a reflected shock tunnel an area ratio of 100 calls for a facility with a 10 cm diameter throat which implies a 30 cm diameter reservoir to maintain a minimum 9:1 area ratio between the reservoir and throat; larger area ratios are preferable. At the higher Mach number regime the limiting facility parameter is reservoir pressure. Reservoir pressures of 10 ksi will permit good simulation up to M =13, 20ksi up to M = 14, and 30 ksi up to M = 15.

In addition to facility reservoir pressure and nozzle area ratio, a third critical test simulation requirement is test gas slug length or steady test time. To perform direct thrust and drag measurements, as well as discrete pressure and heat flux and instream measurements, the steady test gas slug length should be at least three test article body lengths. For a model 3 m long this requires a slug length of 9 m to assure proper flow establishment with a steady flow. For the velocities identified above for Mach 12 and 16 test conditions the total steady flow test time should be at least 2.6 ms and 1.8 ms respectively. As will be

shown later, some segments in the combustor flow path may require test times substantially longer than these to assure proper flow establishment and to permit data acquisition.

With these facility requirements in mind simulation capability of the Ames 16-Inch combustion driven shock tunnel with its 30 cm diameter reservoir and total operational pressure limitation of 10000 psi should provide good simulation to Mach 13 for full scale test articles in the semi-free jet test mode. Extension to higher Mach numbers can be accomplished with diminished total pressure and/or some compromise in matching combustor entrance conditions. Of course, inherent in all high enthalpy facilities that stagnate the flow, there will be test gas contamination due to formation of nitric oxide and dissociated oxygen in the reservoir. As will be shown subsequently, the nitric oxide is present at all Mach numbers, while the dissociated oxygen occurs at discernible levels only at the higher Mach numbers.

While it has been shown that full scale simulation can be achieved at the combustor entrance with a 1 m facility nozzle, this can only be achieved by inclining the combustor to the core flow. For the test configuration selected for the Ames facility, the inlet body surface was aligned with the flow along the nozzle centerline (figure 3). The cowl and combustor were inclined such that the cowl leading edge was just inside the nozzle core flow. The combined length of the cowl and combustor may cause any nozzle segment to extend outside the facility core flow or into the test cabin side walls. To correct this in the Ames facility, the nozzle segment was turned upside down and the flow directed back into the core flow. This change in configuration will have no impact in the inlet and combustor simulation and will still provide valuable performance and CFD validation data for nozzle performance issues.

Inflow Conditions and Calibration

Operation of the Ames 16-Inch Combustion Driven Reflected Shock Tunnel has recently been demonstrated[3] at shock speeds ranging from 2.5 to 3.5 km/s. The plots of total enthalpy and incident shock speed, figure 6, match the flight Mach number conditions expected for a 1000 psf constant dynamic pressure flight trajectory over the Mach 12 to 16.5 range. It has been observed experimentally, using nitrogen as the test gas, that tailored interface operation is approximately achieved for a shock speed near 3 km/s (Mach 14 enthalpy). Tailoring using air as the test gas has not yet been attempted for shock speeds over our demonstrated operating range. Equilibrium interface is established about 2 ms after arrival of the incident shock, and reservoir pressures are nearly constant until the arrival of the expansion wave, approximately 17 ms after incident shock arrival.

Nozzle wall static pressure is currently used on each run as the primary measure of test time[4,5]. A typical time trace, figure 7, shows an initial transient (start-up period followed by a constant pressure period used to acquire and average data. The drop in static pressure at about 6+ ms correlates with the arrival of gas from the driver, and has been confirmed by other measurements including heating rates, oblique shock angle, and OH and H_2O mole fractions. The subsequent constant pressure period to about 17 ms consists largely of driver gases. The observed test time and test gas slug length are shown as a function of flight Mach number. Both test time and slug length decrease with increasing Mach number ranging from a test time of 5 ms at M=12 down to 3.2 ms at M=16, and a test gas slug length of 15 m at M=12 to 12.5 m at M=16, respectively. These test time and flow slug lengths will permit the testing of large sub- and full-scale combustor models, including the possible measurement of total thrust. Somewhat longer test times and slug lengths could be realized with tailored

operation but do not seem necessary for the scramjet tests envisioned.

A further measurement of test time and, additionally, test gas static temperature, is shown in figure 8. Here the nozzle free-stream temperature is shown as measured with a rapid scanning laser absorption system tuned to rotational states of OH. For a few selected tests, the air in the driven tube was saturated with water. The shock heating process resulted in the formation of OH which is detected by the laser absorption diagnostic as it expands in the nozzle. Detectable OH is present only in the driven gas, and test time is measured by observing a decay in the level of OH. The scanning laser diagnostic provides a line-of-site measurement of OH concentration as well as both rotational and translational temperatures. This accurate diagnostic indicates a static temperature of about 1180 K and agrees to within 1% with the temperature prediction obtained using an axisymmetric, nonequilibrium nozzle expansion flow code. The unreduced OH absorption time trace (not shown) indicates a decay in OH mole fraction at the end of the test time consistent with previously shown pressure, heat flux and total radiation data. Recent tests have been performed in which the concentration of H_2O was measured across the nozzle exit. In this case an increase in the level of water indicated the arrival of driver gas. These data corroborate the OH and other data.

Flow contamination results also from test gas dissociation which occurs in the driven gas under the high temperature conditions in the reservoir. These contaminants are manifest in the form of nitric oxide (NO) and atomic oxygen (O). These levels will decrease with increasing reservoir pressure. Once the NO is formed in the reservoir it will continue to exist at essentially unchanged levels as the test gas expands through the nozzle to the facility test section. The atomic oxygen, on the other hand, will undergo some recombination as the test gas expands and cools through the nozzle, and, for long nozzles, the level of O in the test gas will be considerably reduced. Shown in figure 9 are estimates of the atomic oxygen and nitric oxide mole fraction variations with total enthalpy (or flight Mach number) in the reservoir and in the test section. It can be seen that the NO levels in the test section are relatively unchanged with Mach number and, at concentration levels of about 0.05, are about half that computed for the reservoir. Atomic oxygen concentration in the test section increases rapidly with flight Mach number, ranging from very low levels for Mach 12 to about 0.06 at Mach 16. These levels, however, are about an order of magnitude lower than the concentrations in the reservoir, indicating significant recombination during the expansion through the nearly 6 m long facility nozzle.

Spectrally resolved emission measurements of the expanded test gas over the region from the ultraviolet to the near infrared permitted determination of gaseous metal contamination. As a result of careful analysis of this data, high heat capacity material liners and shields were installed in the facility reservoir. This led to significantly reduced levels of flow contaminants and permitted the acquisition of high quality laser imaging flow field data.

Before installing the integrated combustor test article, calibration runs and pre-test CFD analyses were performed. The calibration runs consisted of a large pitot rake mounted across the entire nozzle exit plane. Pressure sensors were uniformly distributed at 2.5 cm intervals across the rake. A shadowgraph of the flow over the central portion of the rake is shown in figure 10. The second probe from the top of the shadowgraph is a hemispherical heat transfer probe and exhibits a different bow shock shape than the pressure probes. There is no evidence of nozzle shocks, or other nozzle disturbances, in the flow. Measured impact pressure profiles are shown in figure 11 for Mach numbers of 12, 14, and 16 for driver pressures of

6000 psi. These represent the full span of the nozzle exit plane, and a uniform core flow of about 70 cm (70% of the nozzle exit diameter) is observed. This is consistent with computational predictions. The standard deviation in impact pressure across this core is less than 10%. Real-gas CFD computations using the quasi one-dimensional NENZF and axisymmetric real gas Navier-Stokes codes were made for conditions corresponding to the facility operating conditions. The results were compared with available calibration data and reasonably good agreement between the data and CFD was found.

Additional facility nozzle exit conditions were computed[6] using a quasi-one-dimensional nonequilibrium nozzle code (NENZF), and an axisymmetric turbulent viscous code with finite rate chemistry (Mozart). Sample computations for Mach 14 simulation conditions are compared in figure 12 for static temperature, static pressure, velocity, and atomic oxygen mole fraction profiles in the nozzle exit plane. For this example the nozzle area ratio was 144 and the reservoir pressure was 326 atmospheres. The static temperature profile is relatively flat at about 1300 K over 93% of the exit diameter of 1 m. The static pressure profile exhibits a slight variation across the nozzle exit plane which is attributed to a slight divergence in the flow profile. Axial velocity shows a boundary layer filling about 30% of the nozzle exit radius, and relatively uniform core flow over 70% of the exit diameter (about 70 cm core flow.) The estimated mole fraction of atomic oxygen is 0.015, less than 10% of the concentration in the reservoir. The agreement between the computed values from the turbulent viscous and quasi-one-dimensional results is reasonable. Across the core flow, the predictions for static pressure agree almost exactly, temperatures agree to within 8%, and mole fraction of atomic oxygen, to within 15%.

For a fixed test article configuration the combustor inflow conditions can be estimated[7]. Shown in figure 13 is a comparison of current combustor inlet test conditions compared to those expected for an ascent vehicle operating at a flight dynamic pressure of q=1000 psf[2]. The test points for equivalent flight Mach numbers of 12, 14, and 16 were determined for the test article shown photographically in figure 2 installed in a semi-free jet mode as shown in figure 3. The conditions shown here are for a cowl fixed at 12 degrees to the flow and the facility configured to provide maximum static pressure at the combustor inlet for facility reservoir pressures of 408 and 680 atm. Under these conditions, the combustor inlet static temperature matches flight conditions at Mach 14, is about 200 K low at Mach 12, and about 400 K high at Mach 16. Inlet velocity is about 200 m/s low, and inlet Mach number, which is relatively constant for the high pressure nozzles selected, drops off with increasing flight Mach number. Overall, however, the simulation of flight conditions is reasonable over the Mach 12 to 16 range.

Using computed nozzle exit conditions from the axisymmetric viscous code with finite rate chemistry[6], flow through the model inlet to the combustor entrance plane was computed for the test Mach numbers of 12, 14, and 16. Shown in figure 14 are the computed combustor inlet profiles across the combustor entrance, from the cowl to the body surface, for velocity, static temperature, pitot pressure, and mole fractions of N_2, N, NO, O_2, and O. Three dimensional Navier-Stokes computations were also performed to assess the influence of three dimensional viscous effects, to confirm the spillage of the vortical corner flow generated by the cowl side strakes and confirm the two-dimensional inflow, and to determine the combustor inlet mass capture. Shown on figure 15 are normalized mass flow contours in the rectangular combustor inlet plane for the test Mach numbers 12, 14, and 16. These exhibit a thickening of the cowl side boundary layer in the central portion of the cowl surface and some modest three-dimensional effects near

the sides and body surface. The body side boundary layer was not included in the three-dimensional simulations but rather was estimated from the two-dimensional solutions.

Shown in figure 16 are surface path lines just above the cowl surface, and particle paths through the combustor inlet, for the Mach 12 test condition[6]. The surface path lines illustrate the strongly three-dimensional vortical nature in the boundary layer induced by the vortices and shocks generated at the leading edge of the cowl/side strake junction. The inlet path lines, however, clearly indicate that the strong vortical flow is spilled off the sides of the combustor inlet and the weak secondary vortices are confined to the cowl surface boundary layer. Overall, the influence of three-dimensional effects on the mass capture was found to increase the two-dimensional mass capture estimates by less than 10 %. Correlations were then developed to provide accurate estimates of mass capture which included real gas and three-dimensional flow effects for the tested configuration.

The inlet flow computations were verified, in part, by comparison with inlet wall static pressure and heat flux measurements. Shown in figure 17 are comparisons of surface heat flux data for several runs at Mach 14 with computed estimates assuming both laminar and turbulent flow. The cowl surface heat flux comparisons clearly indicate a turbulent heating level beginning about 25% downstream from the leading edge. The body surface heat flux appears to be laminar for the entire inlet length. The agreement between the computation and measurements is, in general, excellent.

Instrumentation

The integrated combustor model is fully instrumented with surface pressure (PCB gages) and heat flux (Medtherm coaxial thermocouples) gages. Initially 111 instrumentation ports were located on the inlet, combustor, and nozzle surfaces as shown in figure 18a. Additional surface instrumentation was also installed on the fuel injectors, on the facility walls and external surfaces of the model and supports to monitor the flow in the facility. Subsequent provision has been made to increase the surface instrumentation in the combustor by about a factor of 2 (figure 18b). Accelerometers have also been installed to determine vibrational loads and frequencies of various model and facility components. Further surface instrumentation includes skin friction gages designed and built at VPI[8], installed on the body and cowl inlet and combustor surfaces, and a metric thrust balance designed and built by JHU/APL, installed in the one-sided nozzle. The skin friction gages are particularly useful in assessing combustor drag, and the nozzle metric balance provides a direct measurement of incremental thrust.

In-stream measurements included pitot probes mounted on the body and cowl leading edges and pitot rakes which were installed for selected runs in the combustor exit plane. The in-stream probes will cause downstream flow disturbance, and surface mounted instruments are severely limited in providing information on in-stream thermodynamic and chemistry phenomena. Hence, extensive use is also made of nonintrusive diagnostics, notably laser diagnostic methods, to provide accurate and detailed in-stream information.

Nonintrusive laser diagnostics used in the test program include rapid scanning, multiple line-of-sight laser absorption spectroscopy[9-11]. Specific applications include measurements of O_2 at the combustor inlet and OH at the combustor exit plane and down the nozzle. The rapid scanning capability allows the absorption line shape of several spectral features to be directly recorded at kilohertz frequencies. From the precise line shape data, the properties of mole fraction and temperature can be

determined simultaneously. For the long test times available in the Ames facility, more than ten data points at discrete times can be acquired during a single test. An additional feature of this diagnostic is that beam delivery and detection is accomplished using optical fibers. This feature permits access to restricted internal flow regions. The O_2 diagnostic also includes provision for cross beams for the determination of velocity via the Doppler shift technique. Additionally, multiple line-of-sight laser absorption for H_2O was installed in the combustor exit plane and down the nozzle. Shown in figure 19 is a schematic of the test model showing the optical access port at the combustor exit and down the nozzle. Also shown as an insert is a typical data trace showing the intensity and wave shape of two excited rotational states of the hydroxyl radical. This information is used to determine path integrated mole fraction and translational and rotational temperature of OH simultaneously. A typical trace of water absorption line shape and intensity is shown in figure 20. The water diagnostic, in particular, provides an accurate measure of the combustion product, H_2O, and hence, a direct measure of combustion efficiency.

Double pulse laser holographic images were also obtained across the flow just ahead of the combustor inlet and in the region of the fuel injectors. Images were used to verify inlet performance and to assess near field air/fuel mixing and combustion in the combustor.

The data acquisition system (DAS) consists of 196 channels of high speed transient digitizers capable of recording at sampling rates as high as 5 megasamples per second. The waveform recorders have 12 bit accuracy, variable gain, and 512k record length. The system is augmented with 100 stand-alone channels of instrumentation amplifiers. Additional analog filters, bridge amplifiers/signal conditioners, and instrument-specific conditioning electronics are also available. This state-of-the-art DAS may be expanded to double or triple the present capability if needed for more data collection. The system is controlled by a desk-top computer. Graphical programming is used to control the DAS, drive the instrumentation, and acquire the data. Data processing and graphical output is performed using commercial plotting analysis capability.

Performance Sensitivities

To determine combustor performance with a comprehensive data acquisition system, it is important to have a high spatial density of instruments in the facility and test article and to make highly accurate measurements of the proper flow parameters. Precise measurements of parameters such as static and pitot pressure and mass flux at the facility nozzle exit are critical to proper reduction and analysis of scramjet combustor performance data. Without these data, assessment of inlet mass capture, engine fuel equivalence ratio, and ultimately combustion efficiency and combustor performance cannot be reliably made.

Figure 21 illustrates the sensitivity of key facility performance parameters to small changes in measurement accuracy of facility stagnation temperature and pressure and facility nozzle area ratio. A measurement accuracy of 5% was chosen because this matches a worst case accuracy of a well characterized pressure measurement system. We see in figure 21 that flow pressures and mass flux per unit area show the greatest sensitivity to stagnation pressure and nozzle area ratio. The greatest burden is, therefore, placed on measurement of reflected shock region pressure and on maintenance of nozzle throat integrity. For reservoir pressures in excess of 400 atm and total temperatures approaching 7000 K, careful attention must be paid to pressure gage mounting and maintenance to assure accurate measurements. Multiple gage measurements at the reflected shock region are often required to assure quality data. Similarly, nozzle throat wear can be significant at these

conditions. Proper choice of throat material and frequent replacement is necessary for tolerance control of nozzle area ratio.

It is also important to accurately measure the proper flow parameters in the scramjet to determine combustor efficiency and performance. Given the existing technology and methodology to accurately measure pressure in the combustor as well as the CFD capability to simulate 3-D scramjet internal flow pressure, a natural analytical process to evaluate combustor performance could be accomplished via comparison of measured and computed pressure. For Mach numbers at or below 10, the pressure rise due to combustion is large enough that this comparison is viable. For the Mach number range covered in scramjet tests at the 16-Inch Shock Tunnel, the pressure rise due to combustion is small compared to tare and mixing values. Shock structures in the combustor region also complicate this analysis technique. Shocks initiated by fuel injectors impinge on the combustor surface at locations which vary relative to the positions during tare shots for cases of mass addition (as with fuel addition during injection) and for energy addition (as with heat release during combustion). As shown in figure 22, measurement of overall pressure rise due to mixing or due to combustion is difficult to estimate. Integrating pressure along the combustor eliminates some of the ambiguity and clearly demonstrates a measurable pressure rise. Resolution, however, is lost and comparison with CFD becomes less accurate. It is better to make a direct measure of combustor performance or efficiency. Performance or thrust can be directly measured with the metric balance. Combustion efficiency can best be determined by measuring the mole fraction of water at the combustor exit. Comparison of exit pressure with exit water mole fraction as a direct measure of combustion efficiency for a nominal 5% measurement error is shown in figure 23. A 5% error in the measurement of pressure leads to about a 35% uncertainty in the assignment of combustion efficiency, whereas a 5% error in the measurement of water vapor mole fraction leads to about a 5% uncertainty in assignment of combustion efficiency.

Test Results

A schematic of an integrated combustor installed in a test cabin at the exit of the 16-Inch Shock Tunnel nozzle is shown in figure 24. As mentioned earlier, the length of the model is of the order of 3 m. To assure proper flow establishment the steady test gas should be at least three body lengths (~ 9 m). Shown in figure 7 were measured steady test gas slug lengths ranging from 15 m at Mach 12 to 12.5 m at Mach 16. Including the facility start up transient the total slug lengths, before the arrival of driver gas contamination, ranges from 24 m at Mach 12 to 19 m at Mach 16. Corresponding test times range from 5 ms at Mach 12 to 3.2 ms at Mach 16. These test gas slug lengths and steady test time should clearly be sufficient to establish a steady flow for the entire combustor length for a period long enough to collect and average data. The data averaging period used in all the tests in the Ames facility is 2 ms.

Typical data traces corresponding to several key positions in the flow path are shown in figures 25 through 27. The data selected for illustration are pressure vs. time traces for a Mach 12, 14, and 16 test condition respectively. Included in each figure are pressure vs. time traces at 1) the shock tunnel reservoir, 2) the facility nozzle exit, 3) the cowl inlet surface, 4) the ramp fuel injector base, 5) the combustor exit, and 6) the nozzle surface. The zero time point for each of the six positions has been shifted to coincide with the position of the slug of test gas. The scales on the pressure traces are not indicated and differ significantly from point to point. Taking, for example, the Mach 14 data it can be seen in figure 26 that the reservoir pressure after the start-up transient is steady for about 6 ms. The facility nozzle exhibits a somewhat

longer start-up transient but also shows better than 5 ms of steady pressure. The cowl inlet pressure trace is similar to the nozzle exit behavior. The ramp injector base pressure (4), however, exhibits a distinctly different behavior. The startup transient is exacerbated by the fact that fueling was initiated before the facility start-up and the longer time required to establish the recirculating flow in the base region. Injector base pressurization, which may tend to mitigate this transient was not implemented in this particular test run. Never-the-less, there appears still to be adequate steady flow to establish a 2 ms data averaging period. The base pressure appears to degrade earlier in the run than do the pressures at other parts of the flow path, indicating a greater sensitivity to possible flow contamination or back pressurization issues. The size of the averaging period of 2 ms is based on the available steady pressure time in the base flow region which is believed to be the most sensitive to start-up transients and driver gas arrival. The pressure trace at the combustor exit shows a time behavior similar to the injector base pressure trace, indicating that the steady test time ends abruptly at the same point in time. Pressure levels, however, differ considerably from the fuel injector base pressure. Finally, the nozzle pressure trace exhibits a similarly long flow establishment period but appears insensitive to end of the run variations. Clearly, however, all pressure traces indicate sufficient steady flow over the same time interval to support a consistent and well defined 2 ms data averaging period.

Steady behavior within the established test time was similarly observed with all other instrumentation (thermocouples, skin friction gages, metric balance, and absorption diagnostics.) This is particularly encouraging information since these instrumentation applications were uniquely applied to scramjets in the Mach number range of 12 to 16 for the first time. A comprehensive test matrix, which involved variations in fueling schedules and included tare (no fuel) and mixing (helium instead of hydrogen) runs was acquired to determine combustor performance and efficiency. Heavy reliance was made on extensive CFD analysis, including both quasi-one-dimensional analysis codes and fully three-dimensional reacting flow codes to assess the shock dominated flow structure and estimate combustor performance parameters. Several of the new instrumentation systems (skin friction, metric balance, and water absorption) have contributed first-time ever data valuable for combustor performance assessment.

Future Upgrades

The facility as configured in figure 28a is currently operated at a 6000 psi driver condition. Operation at 8000 psi has been achieved but is typically accompanied by some unsteadiness in reservoir pressure. It is believed that routine operation with a driver pressure of 10,000 psi is readily achievable with straight forward modification to the gas loading and ignition systems and the main diaphragm clamp. These planned changes will also improve flow quality and turn-around time, as well as reduce operation costs. Additional modifications are possible to increase the operational pressure to 30,000 psi or to increase model scale[12]. Increase in total pressure can be accomplished in either of two ways: (1) replace the 0.3 m dia. straight driven tube with a tapered driven tube (figure 28b), or (2) replace the combustion driver with a resistive heated driver and new main diaphragm clamp (figure 28c). Compared to the present configuration, the first option may restrict model size for the lower Mach number operation, but should not affect scale at the higher (M>13) Mach numbers. Facility scale can also be increased for testing up to Mach 14 simply by installing a larger nozzle, test section, and exhaust tank (figure 28d).

Shown in figure 29 is the predicted performance achievable by different modifications to the existing reflected

shock tunnel configuration. Combustor entrance parameters illustrated include static pressure, static temperature, velocity, and O_2 mole fraction. The reflected shock tunnel is assumed used in a semi-free jet mode. Contrary to the results shown in figure 13, in which the cowl is fixed at 12 degrees to the flow and the facility configured to provide maximum static pressure, the results in figure 29 are determined by matching combustor entrance temperature and determining the resulting entrance static pressure. The entrance static pressure can be directly reduced by reducing the driver pressure. Increased entrance static pressure can be realized by relaxing the requirement to nearly match temperature (the method used to produce the results in figure 13). The figures show that it is possible to provide good simulation up to Mach 18 using a large reflected shock tunnel in semi-free jet mode with a resistive heated driver or a 3:1 tapered driven tube. Simulation to Mach 17 can be matched with a 2:1 tapered driven contraction, and to Mach 15 with the current configuration.

Large, sub scale models of complete flight articles can be accommodated by enlarging the existing facility nozzle and test section. With total reservoir pressure of 30,000 psi, simulation up to flight Mach numbers of about 14 is possible and test time can be maximized by operating the reflected shock tunnel in tailored interface mode. Illustrated in figure 30 is a schematic of a 1/4 scale flight vehicle mounted in an upscaled facility. It is possible to simulate flight dynamic pressure with test times from about 10 to 20 ms with tailored operating conditions. Test Reynolds number scales directly with test article scale and should be sufficient to assure fully developed turbulent flow at the combustor entrance.

CONCLUDING REMARKS

A capability for performing large-to-full scale integrated scramjet tests in a large reflected shock tunnel over the flight Mach number range of 12 to 16 has been demonstrated. With this method it is possible to measure, to a high degree of certainty, the combustion efficiency and incremental thrust and to assess the relative performance of different design concepts. Also identified were straight-forward techniques to further enhance the ground test capability to simulate higher flight dynamic pressure, a wider flight Mach number range, and larger test articles, including subscale models of the complete propulsion flow path. Instrumentation for high Mach number pulse facility testing has been developed and demonstrated that, when coupled with advanced CFD analysis, can provide a data base to greatly increase our understanding of scramjet technology and performance for flight Mach numbers greater than 10.

Acknowledgments

Substantial participation and contributions to this work have been made by members of the Aerothermodynamics and Thermophysics Facilities Branches of the Thermosciences Division at the NASA Ames Research Center and the Hypersonic Vehicles Office at the NASA Langley Research Center, by support service contractors from the General Applied Science Laboratories, Inc., Sterling Software, Inc., The Thermosciences Institute of Eloret, Calspan Corporation, MCAT Institute, and by collaborators from Pratt & Whitney, the Virginia Polytechnic Institute, Stanford University, San Jose State University, and the Johns Hopkins University Applied Physics Laboratory.

References

[1] Billig, F. S., Waltrup, P. J., Gilreath, H. E., White, M. E., Van Wie, D. M., and Pandolfini, P. P., "Proposed Supplement to Propulsion System Management Support Plan," JHU/APL-NASP-86-1, July 15, 1986.

[2] Billig, F. S., "Combustion Processes in Supersonic Flow," AIAA J. Propulsion, Vol. 4, No. 3, May-June 1988, pp. 209-216.

[3] Cavolowsky, J. A., Loomis, M. P., Newfield, M. E., and Tam, T. C., "Flow Characterization in the NASA Ames 16-Inch Shock Tunnel," Paper 92-3810, 28th AIAA/SAE/ASME/ASEE Joint Propulsion Conference, July 6-8, 1992, Nashville, TN.

[4] Cavolowsky, J. A. and Newfield, M. E., "Laser Absorption Flow Diagnostics for Use in Hypersonic Ground Based and Flight Experiments," Paper 92-5088, 4th AIAA International Aerospace Planes Conference, December 1-4, 1992, Orlando, FL.

[5] Cavolowsky, J. A., Newfield, M. E., and Loomis, M. P., "Laser Absorption Measurements of OH Concentration and Temperature in Pulsed Facilities," AIAA Journal, Vol. 31, No. 3, March 1993, pp. 491-498.

[6] Papadopoulos, P., Tokarcik-Polsky, S., Venkatapathy, E. and Deiwert, G. S., private communication, abstract entitled "The NASA Ames 16-Inch Shock Tunnel Nozzle Simulations and Experimental Comparison," submitted for 33rd AIAA Aerospace Sciences Meeting, January, 1995.

[7] Loomis, M. P., "Issues with Regard to High Speed Combustor Testing in Short Duration Facilities," unpublished paper presented at the 4th AIAA International Aerospace Planes Conference, Dec. 1-4, 1992, Orlando, FL.

[8] Bowersox, R., Schetz, J. Chadwick, K. and Deiwert, G., "Direct Measurements of Skin Friction in Hypersonic High Enthalpy Impulsive Scramjet Experiments," Paper 94-0585, 32nd AIAA Aerospace Sciences Meeting & Exhibit, Jan. 10-13, 1994, Reno, NV.

[9] Strawa, A. W. and Cavolowsky, J. A., "Development of Non-Intrusive Instrumentation for NASA-Ames' Ballistic Range and Shock Tunnel," AIAA Paper 90-0628, 28th AIAA Aerospace Sciences Meeting, January 8-11, 1990, Reno, NV.

[10] Tam, T. C., Brock, N. J., Cavolowsky, J. A., and Yates, L. A., "Holographic Interferometry at the NASA-Ames Hypervelocity Free-Flight Aerodynamic Facility," Paper 91-0568, 29th AIAA Aerospace Sciences Meeting, January 7-10, 1991, Reno, NV.

[11] Newfield, M. E., Loomis, M. P., Gopaul, N. K. J. M., Ghorbani, A., Kowalski, T. R., and Cavolowsky,. J. A., "Optical Fiber Applications of Laser Absorption Diagnostics in Scramjet Combustors," Paper 94-0386, 32nd AIAA Aerospace Sciences Meeting, January 10-13, 1994, Reno, NV.

[12] Bogdanoff, D. W., Wilson, G., and Park, C., "Options for Upgrade of Ames 16-Inch Shock Tunnel," Paper 94-0545, 32nd, AIAA Aerospace Sciences Meeting, January 10-13, 1994, Reno, NV.

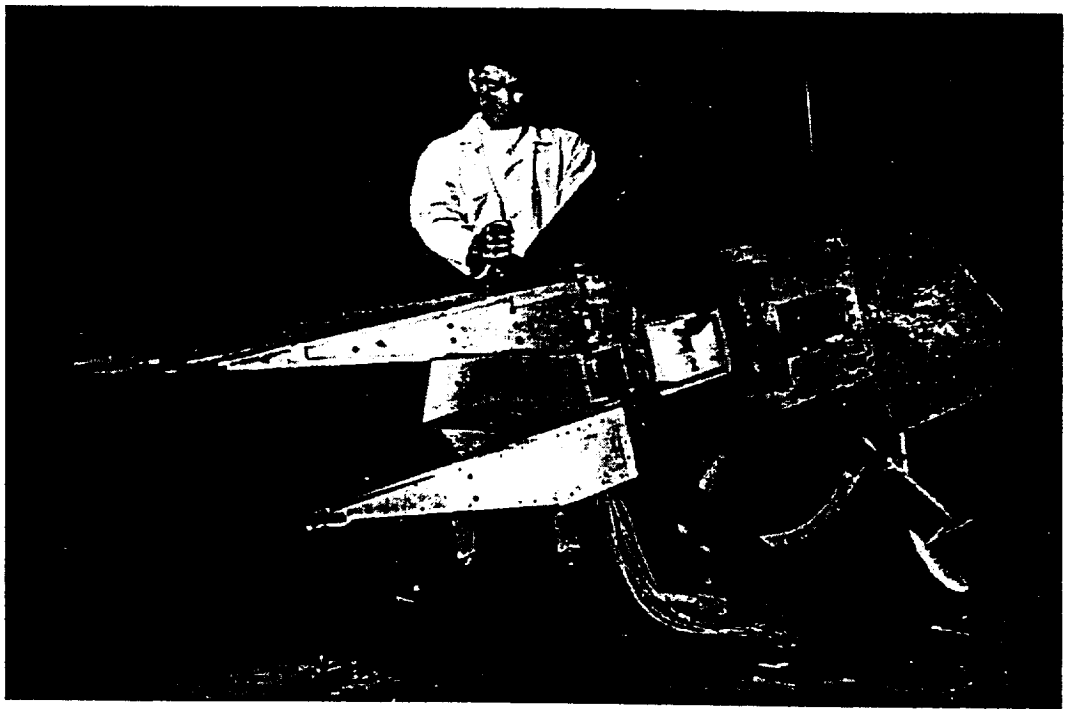

Fig. 2 Full-scale integrated scramjet combustor test article prepared for the Ames 16-Inch Combustion-Driven Shock Tunnel

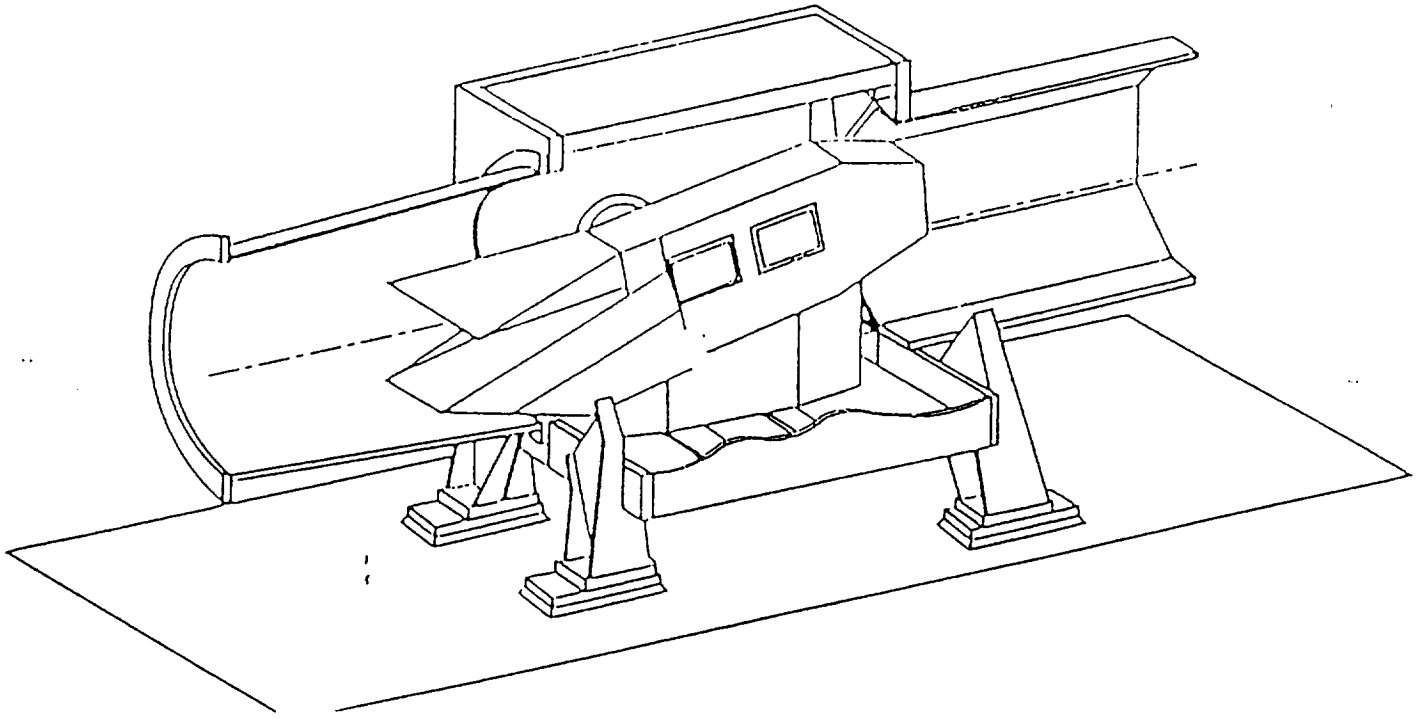

Fig. 3 Semi-free jet installation of integrated combustor model installed in the Ames 16-Inch Combustion-Driven Shock Tunnel

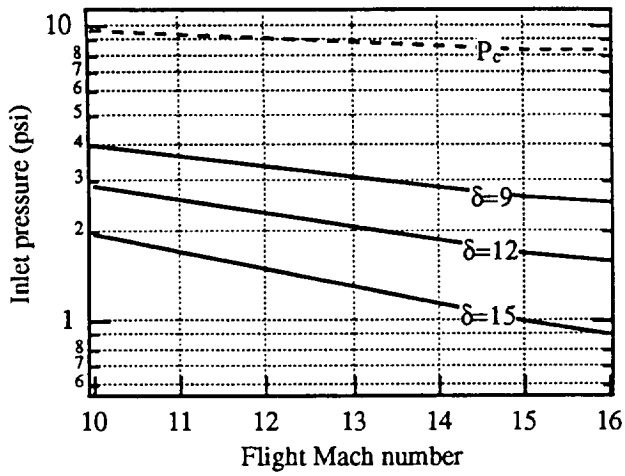

a) Inlet pressure simulation

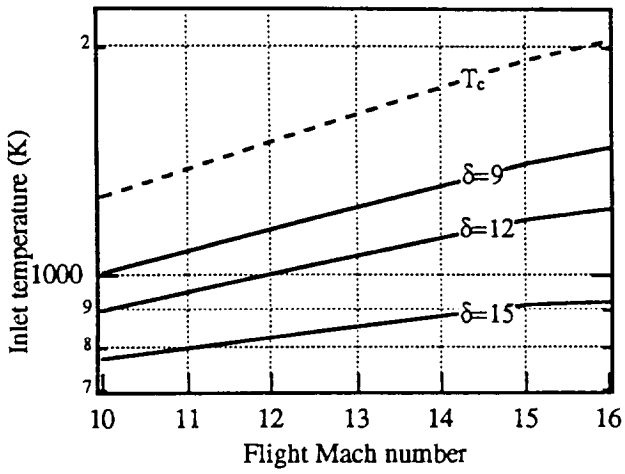

b) Inlet temperature simulation

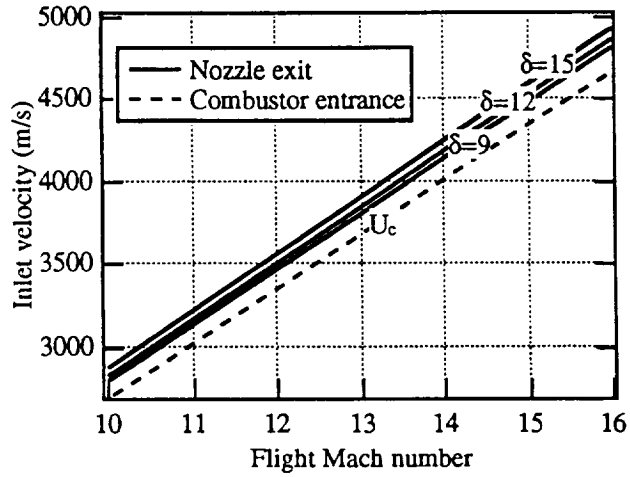

c) Inlet velocity simulation

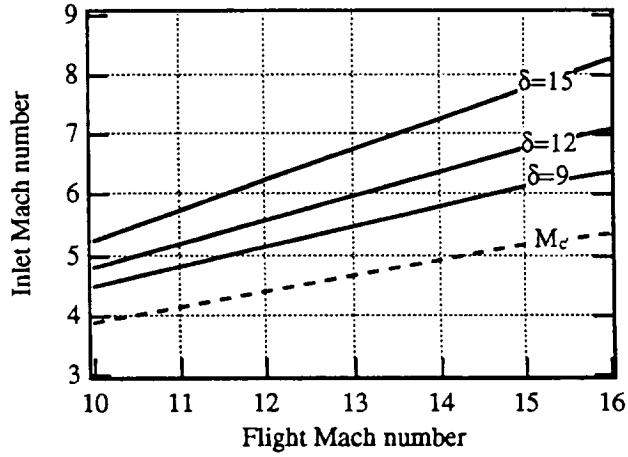

d) Inlet Mach number simulation

Fig. 4. Combustor entrance parameter simulation requirements; Q=1000 psf

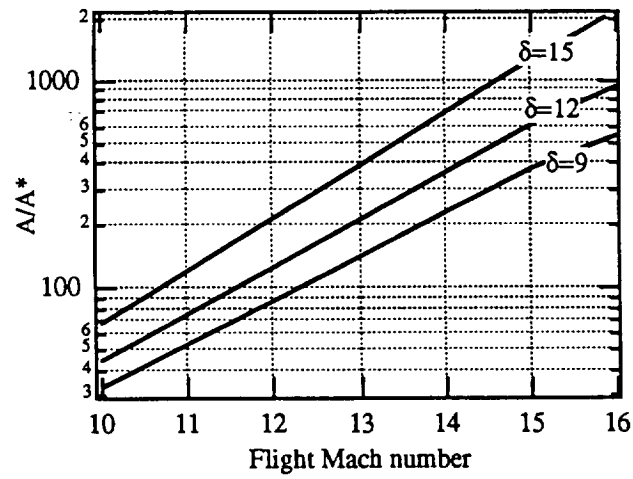

a) Nozzle expansion ratio requirements

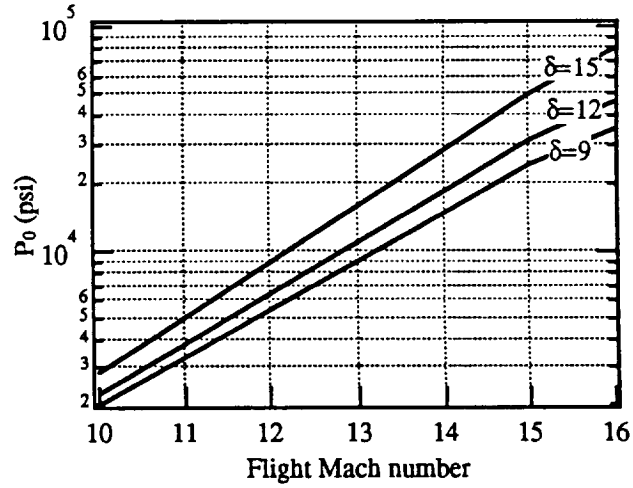

b) Reservoir pressure requirements

Fig. 5. Facility requirements for combustor entrance simulation; Q=1000psf, δ = cowl angle

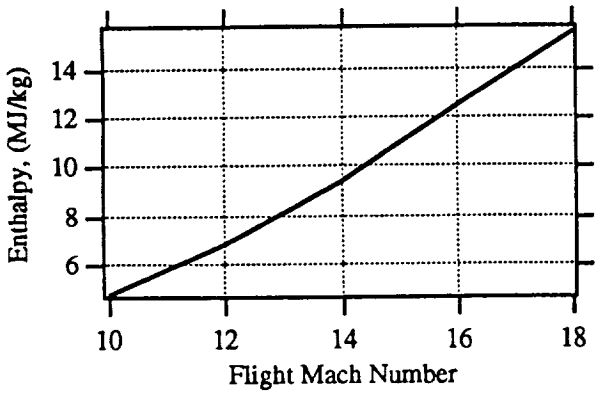

a) Total enthalpy vs. flight Mach number

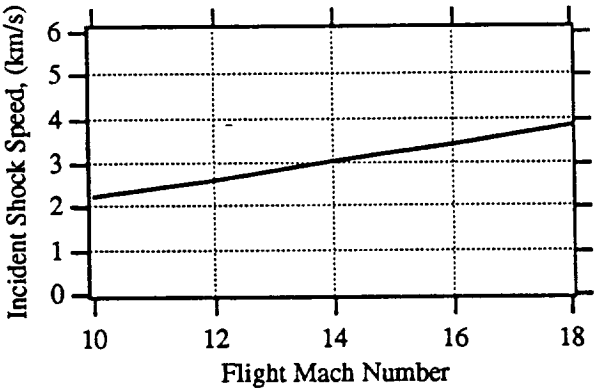

b) Incident shock speed vs. flight Mach number

Fig. 6. Flight Mach number simulation

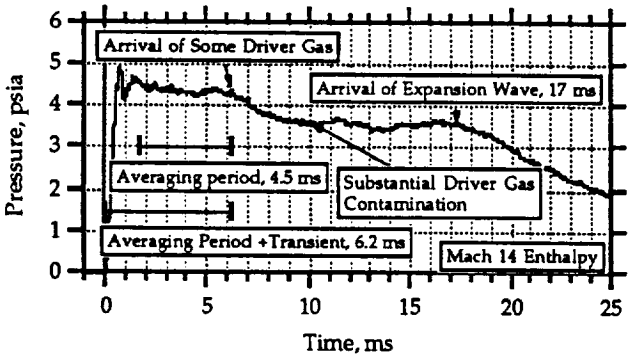

a) Test section pressure history; M=14

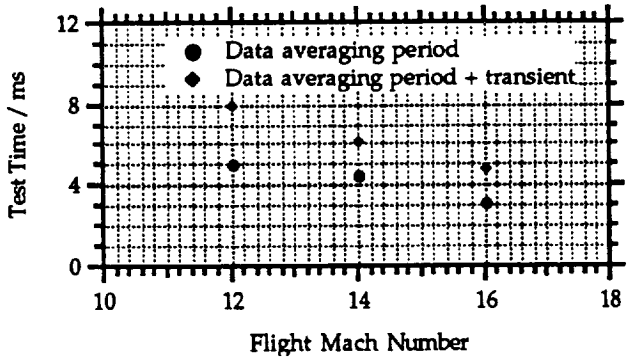

b) Test time variation with Mach number

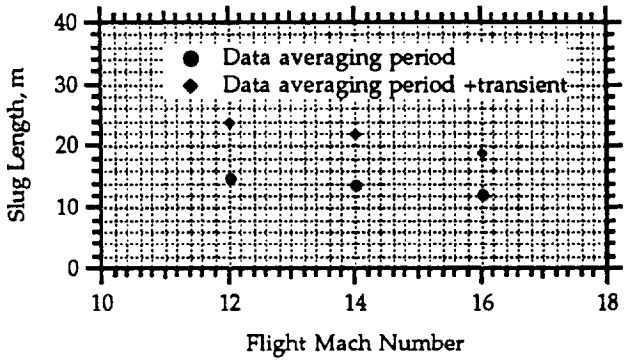

c) Test gas slug length variation

Fig. 7. Test time characterization of Ames 16-Inch Shock Tunnel

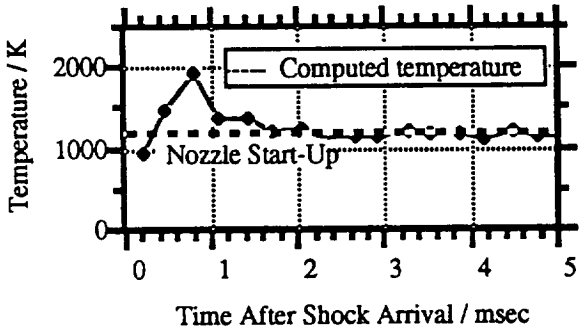

Fig. 8 Test section static temperature. OH absorption diagnostic and computation for M=14

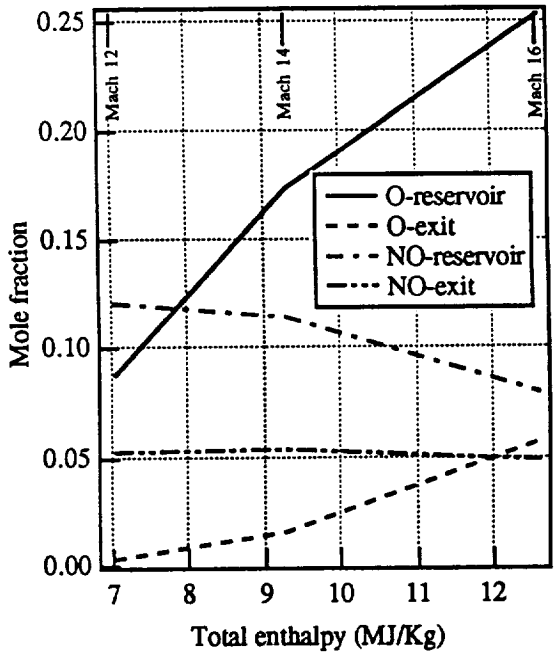

Fig. 9 Computed NO and O mole fraction in shock tunnel reservoir and nozzle

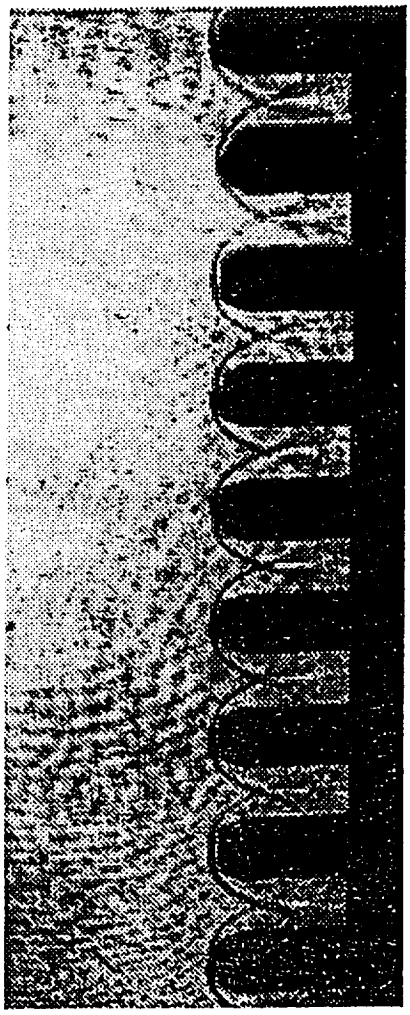

Fig. 10. Shadowgraph of central section of calibration rake at Mach 14 simulation conditions

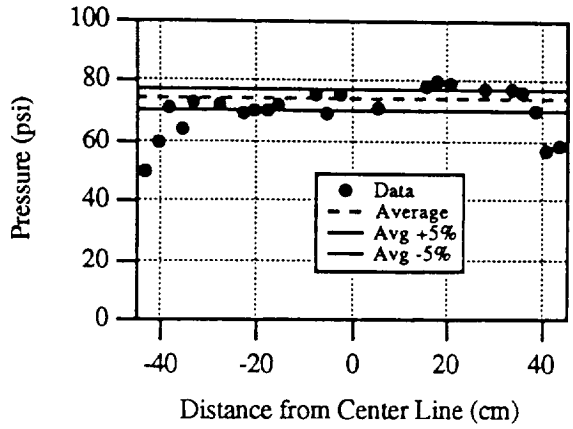

a) Mach 12, T_O = 4800 K, p_O = 5400 bar, A/A* = 124, computed pressure = 77.9 psi

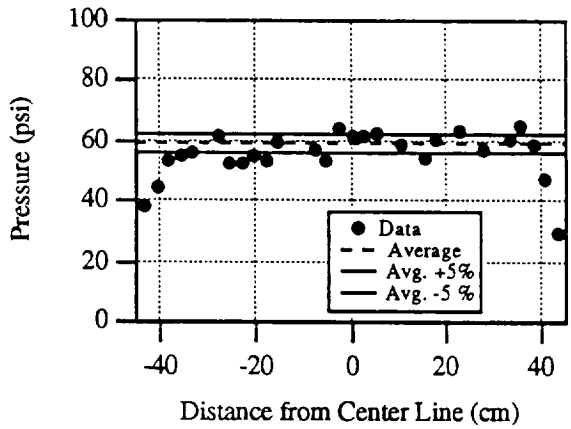

b) Mach 14, T_O = 5900 K, p_O = 5250 bar, A/A* = 144, computed pressure = 67.8 psi

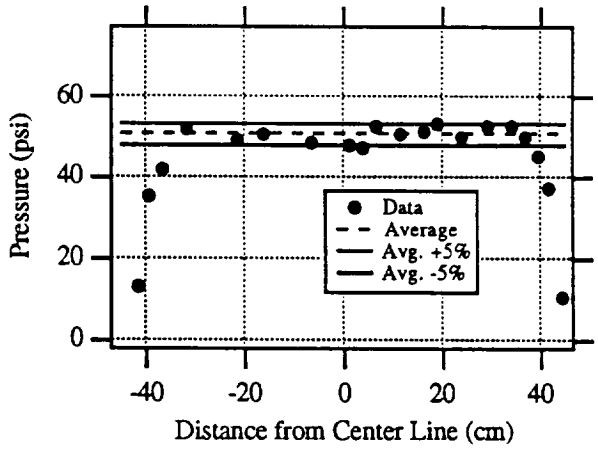

c) Mach 16 , T_O = 7100 K, p_O = 5100 bar, A/A* = 169, computed pressure = 51.7 psi

Fig. 11. Measured and computed nozzle exit pitot profiles

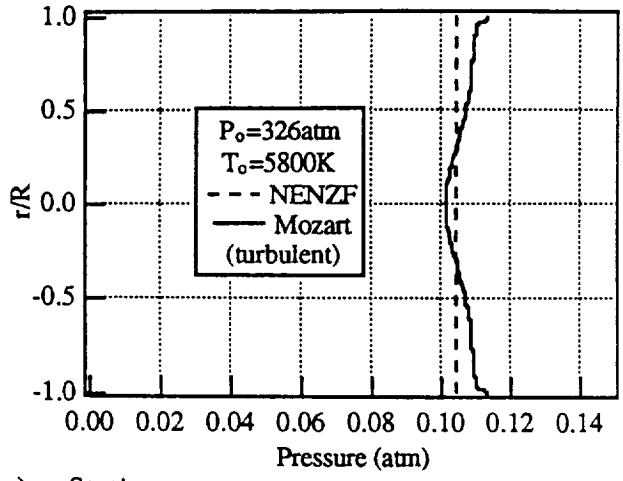

a) Static pressure

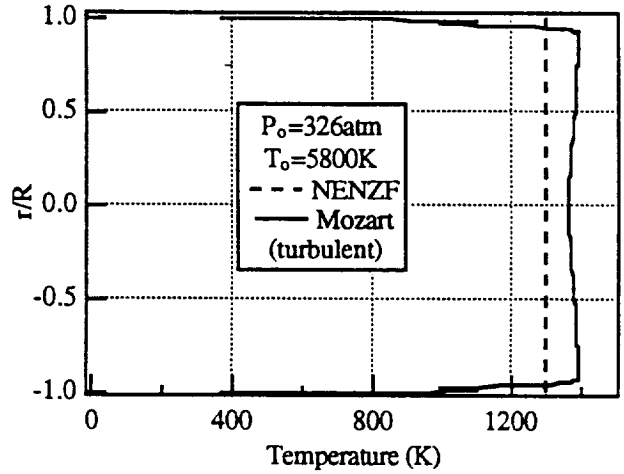

b) Static temperature

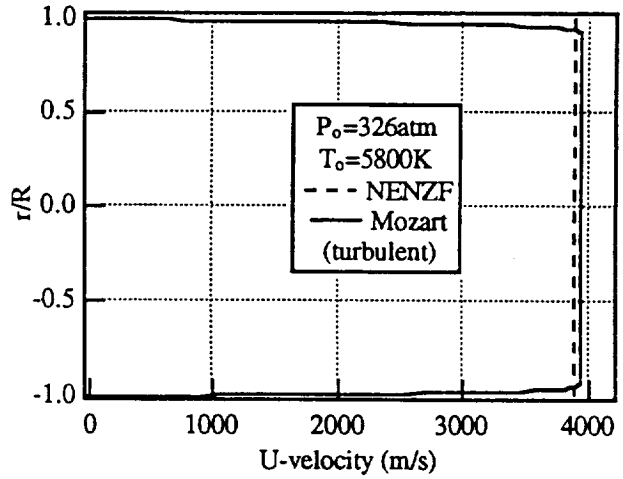

c Axial velocity

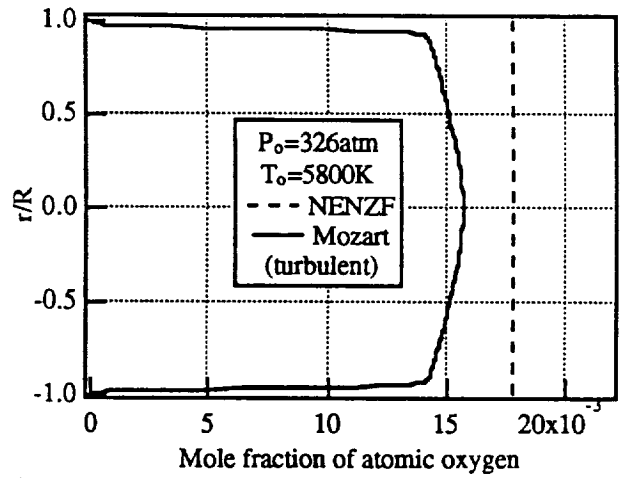

d) Atomic oxygen mole fraction

Fig. 12. Computed nozzle exit profiles

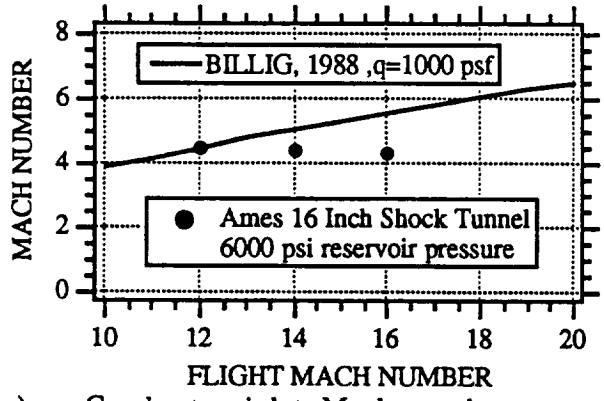

a) Combustor inlet Mach number

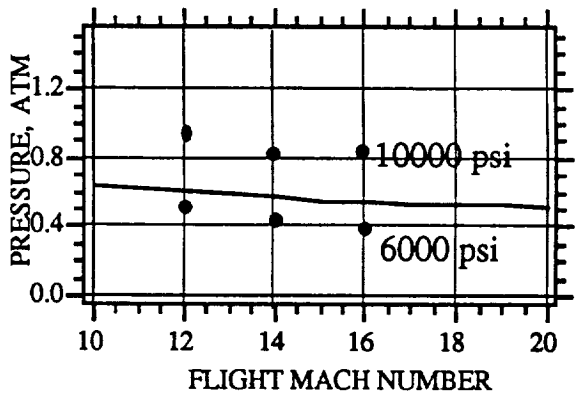

c) Combustor inlet static pressure

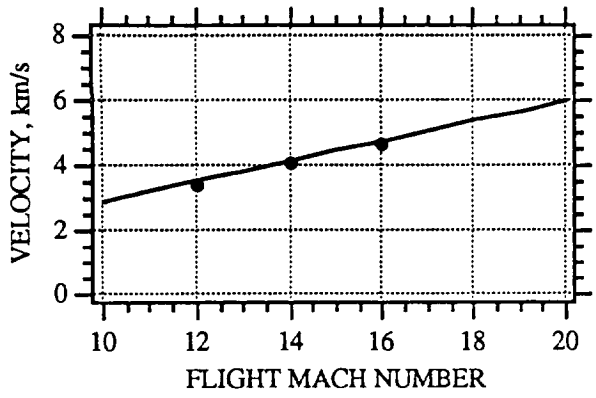

b) Combustor inlet velocity

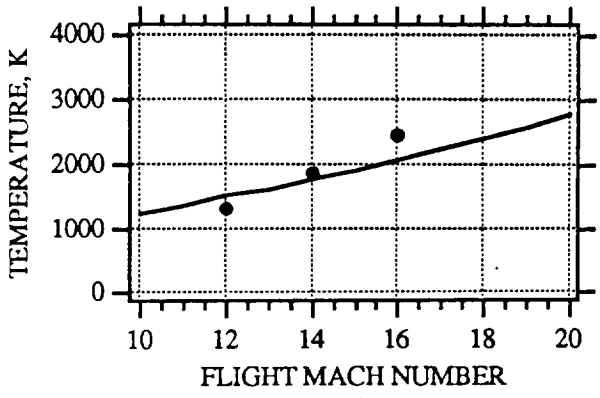

d) Combustor inlet static temperature

Fig. 13. Combustor inlet simulation for fixed test article configuration compared with 1000 psf flight trajectory

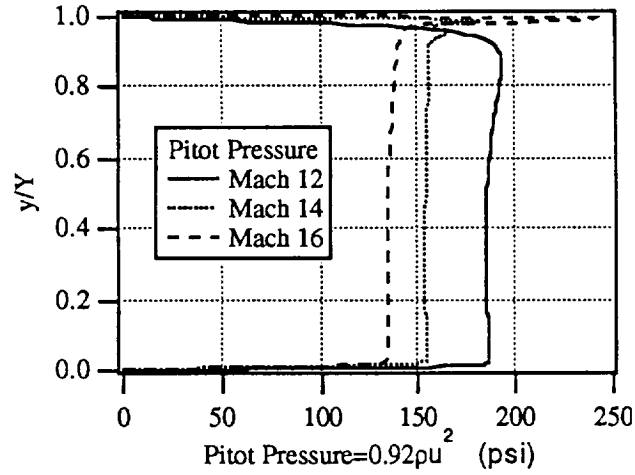

a) Combustor inlet pitot profiles

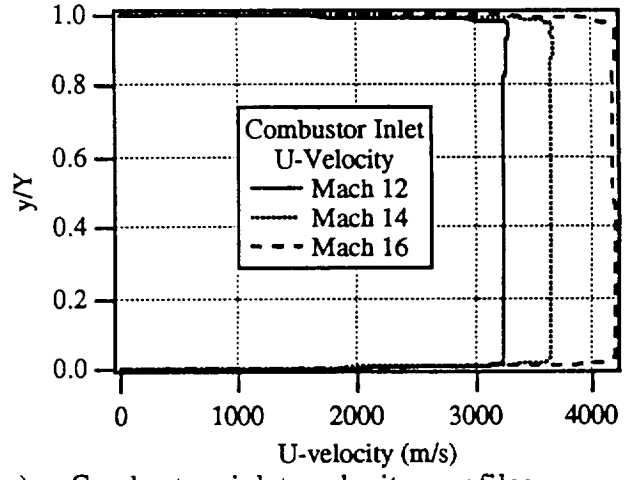

e) Combustor inlet velocity profiles

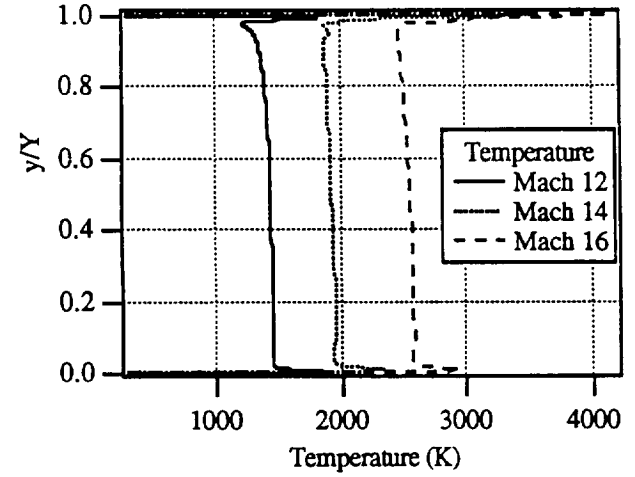

b) Combustor inlet temperature profiles

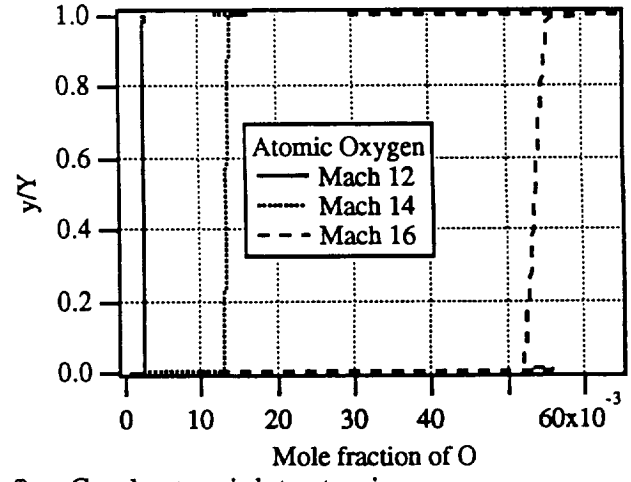

f) Combustor inlet atomic oxygen profiles

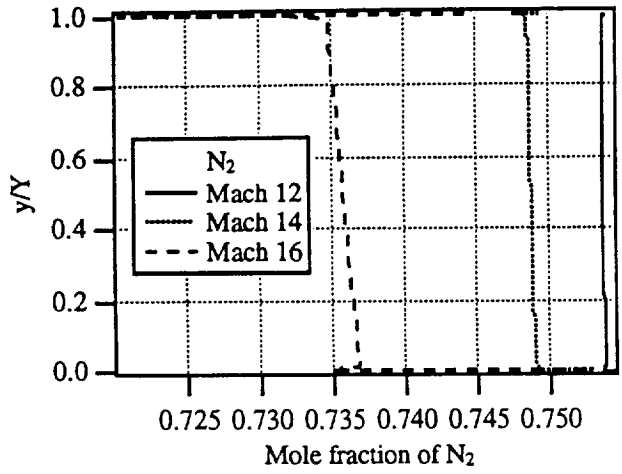

c) Combustor inlet nitrogen profiles

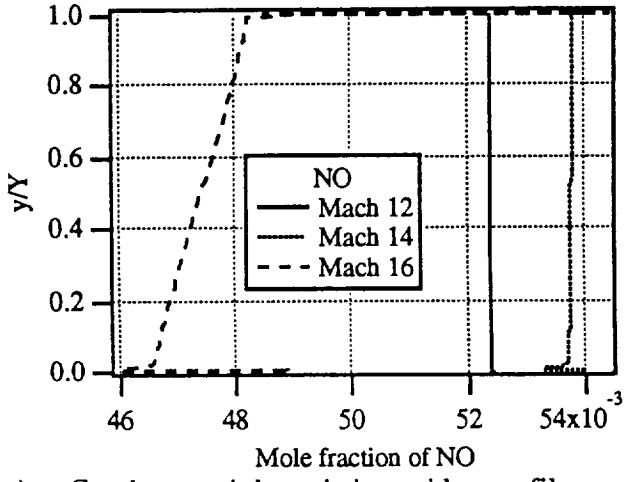

g) Combustor inlet nitric oxide profiles

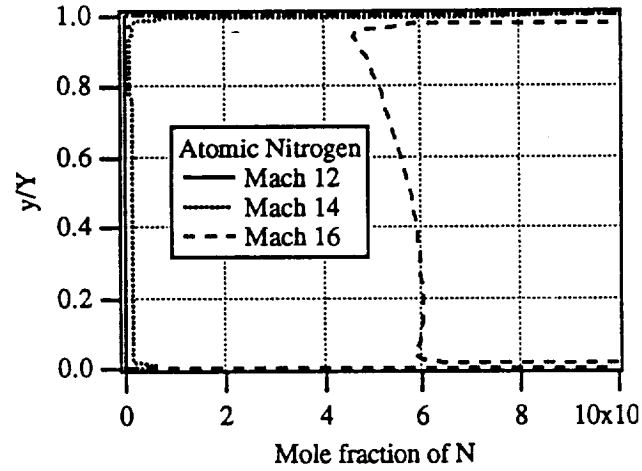

d) Combustor inlet atomic nitrogen profiles

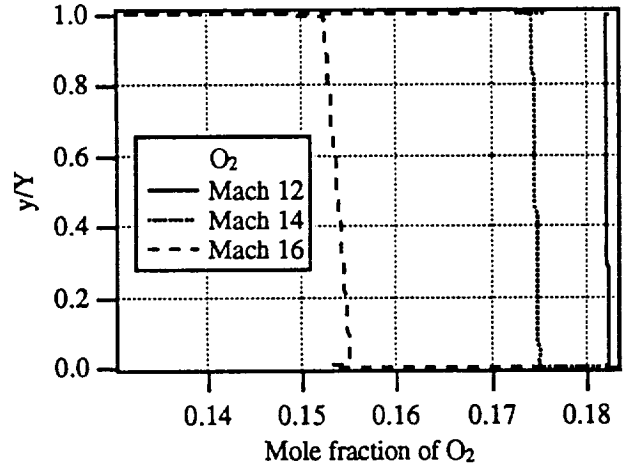

h) Combustor inlet oxygen profiles

Fig. 14 Computed combustor inlet profiles

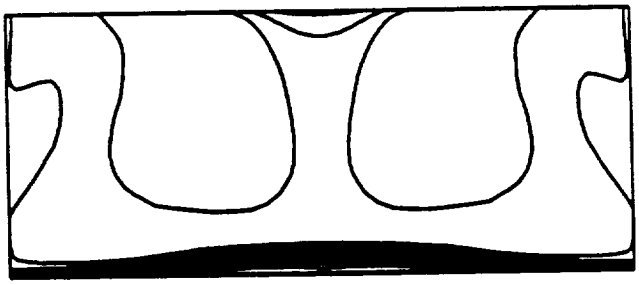

a) Mach 12

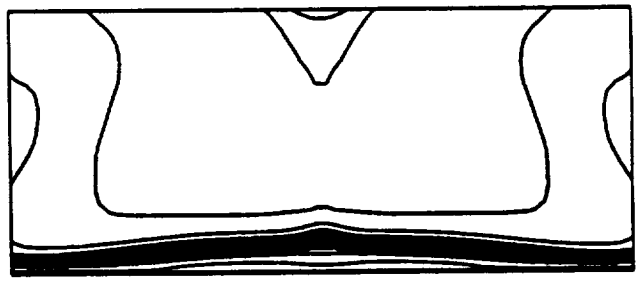

b) Mach 14

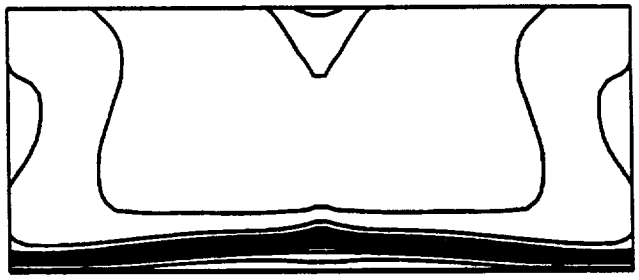

c) Mach 16

Fig. 15. Computed combustor inlet mass flow contours

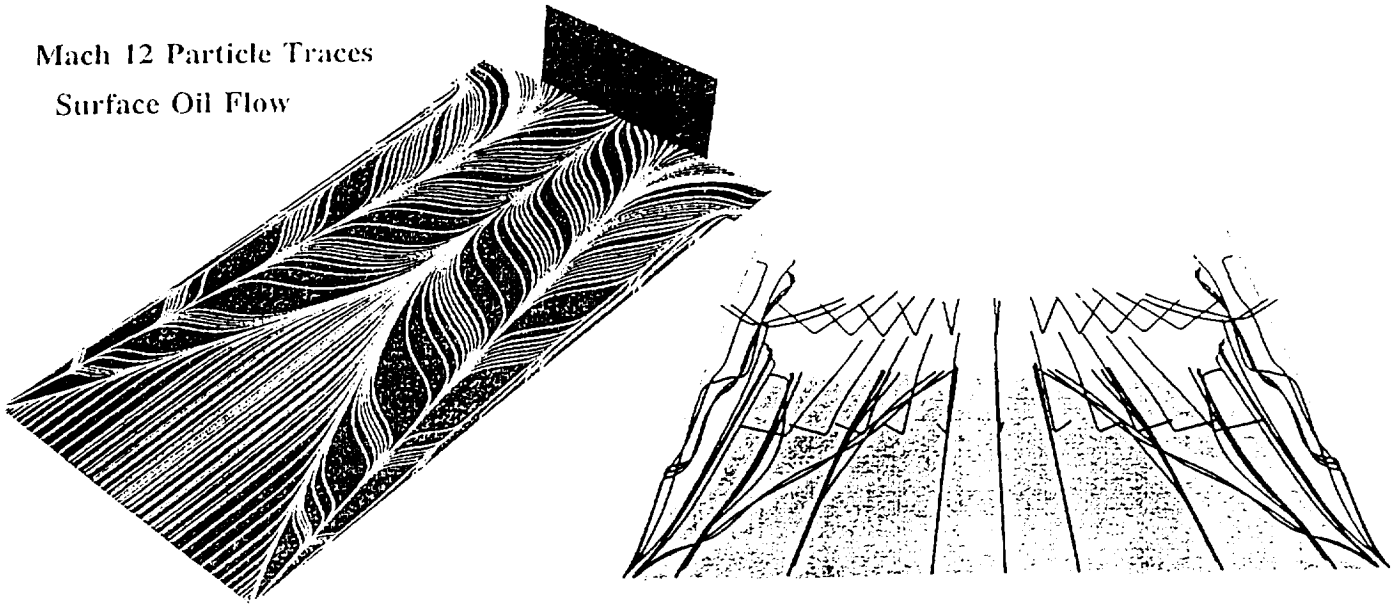

a) Cowl surface path lines

b) Inlet particle paths

Fig. 16 Computed inlet flow path. M=12

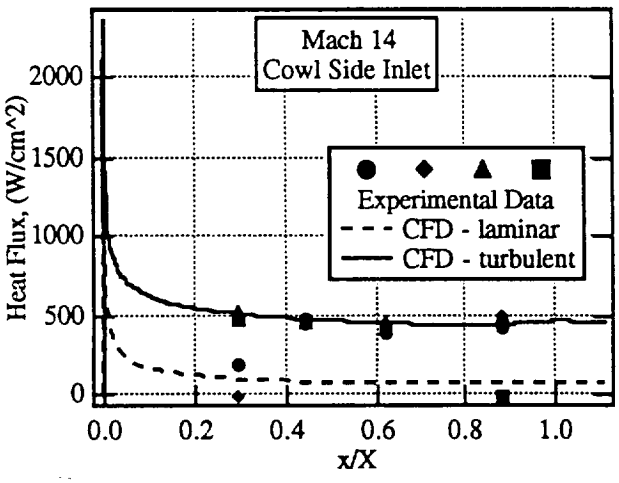

a) Cowl side

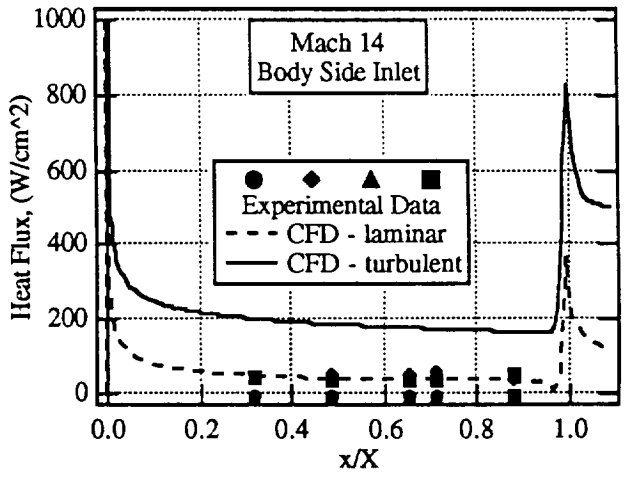

b) Body side

Fig. 17. Computed and measured inlet heat flux. M=14

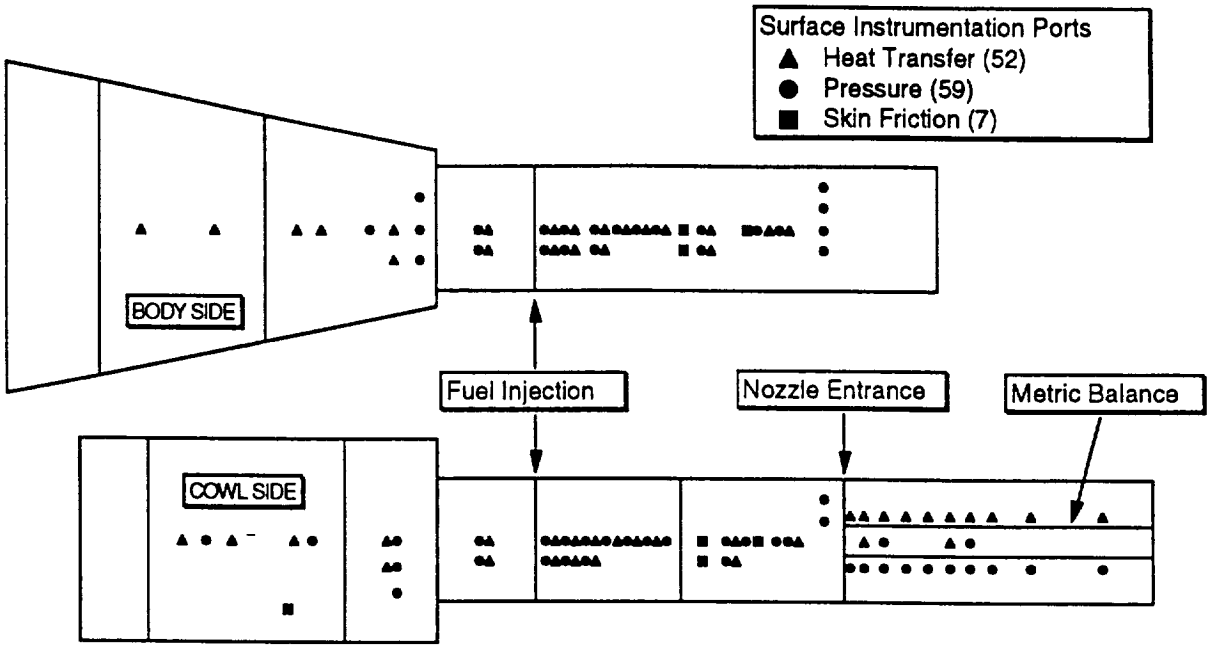

a) Initial instrumentation layout

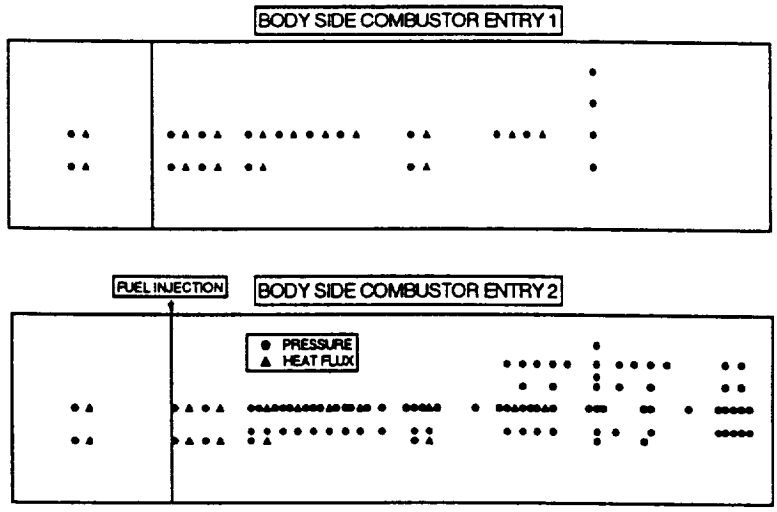

b) Augmented instrumentation layout in combustor

Fig. 18. Surface instrumentation distribution on integrated scramjet test article

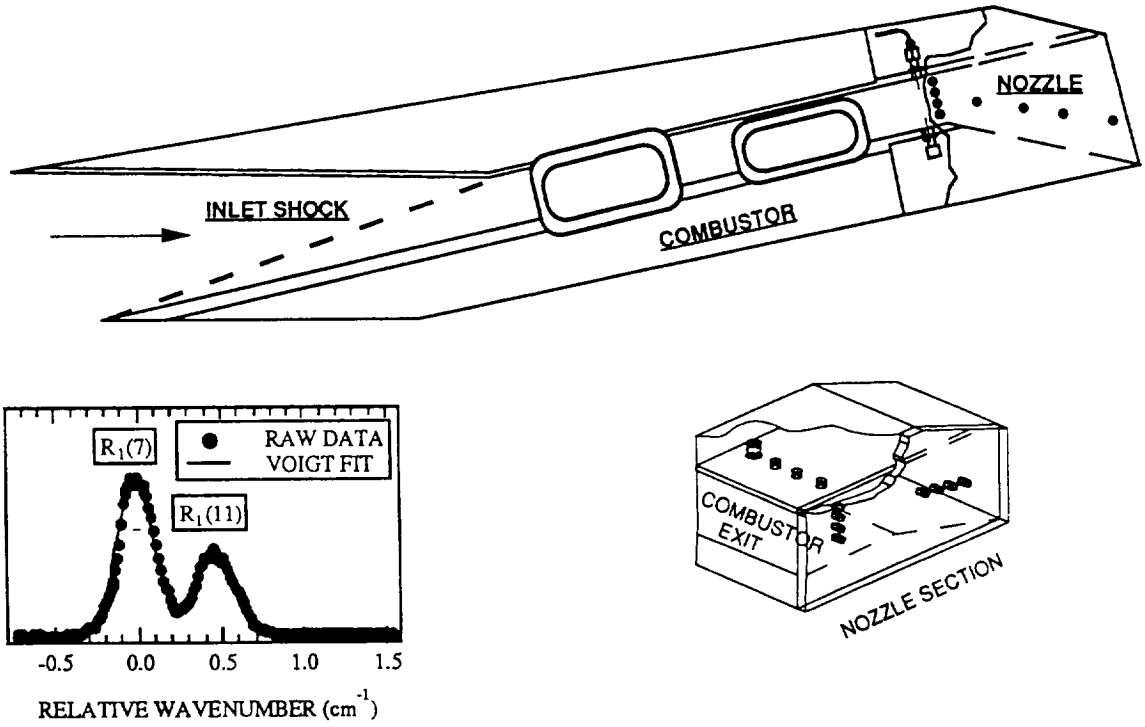

Fig. 19 Schematic of line-of-sight optical diagnostic access in combustor exit and nozzle. Typical OH absorption profiles shown in inset.

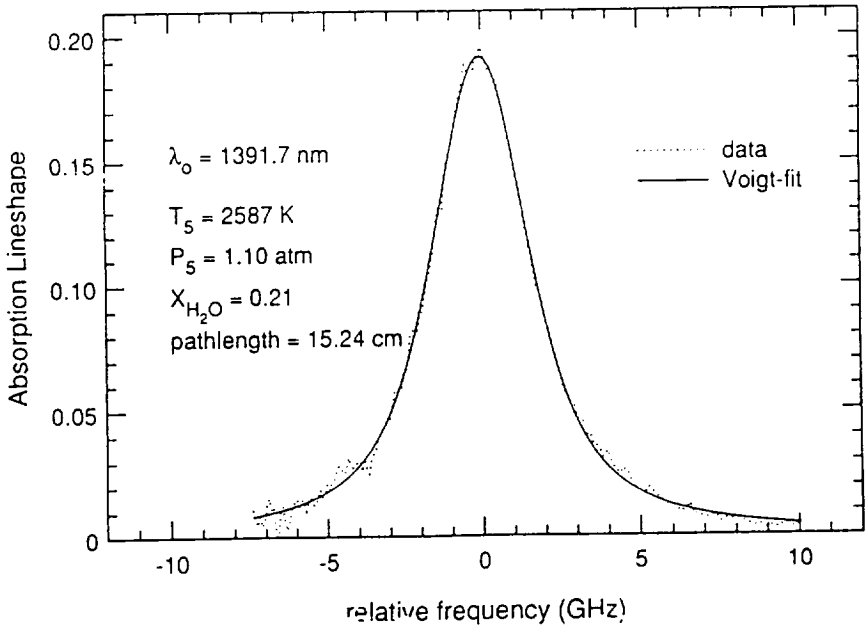

Fig. 20 Line-of-sight H_2O absorption line shape in shock heated flow

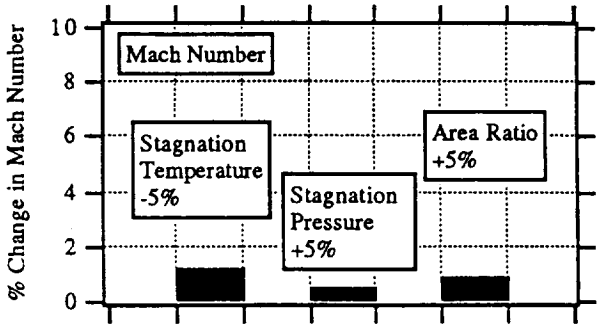

a) Mach number sensitivity

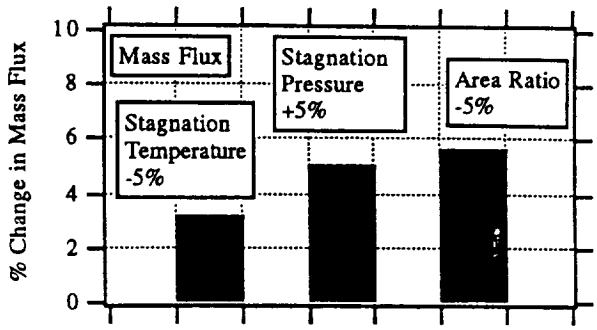

c) Mass flux sensitivity

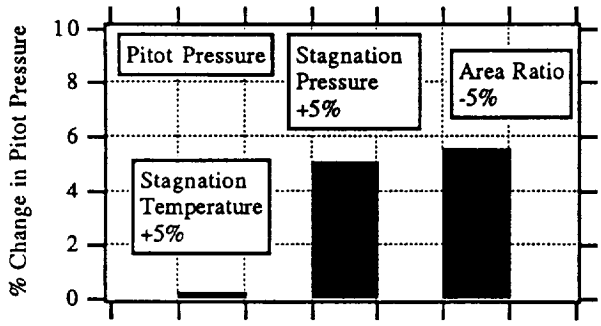

b) Pitot pressure sensitivity

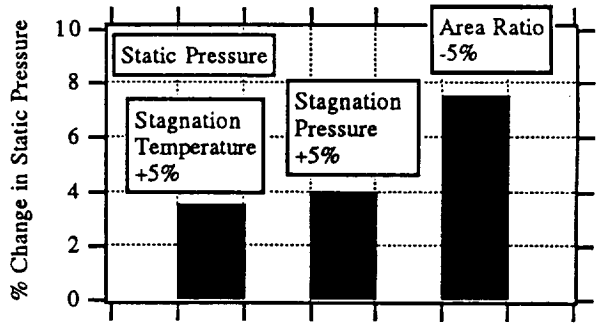

d) Static pressure sensitivity

Fig. 21 Sensitivities of combustor flow properties

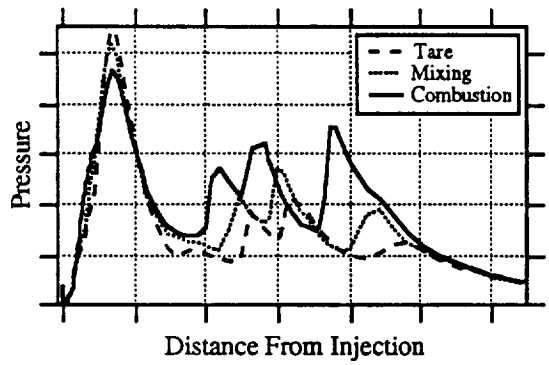

a) Computed pressure variation

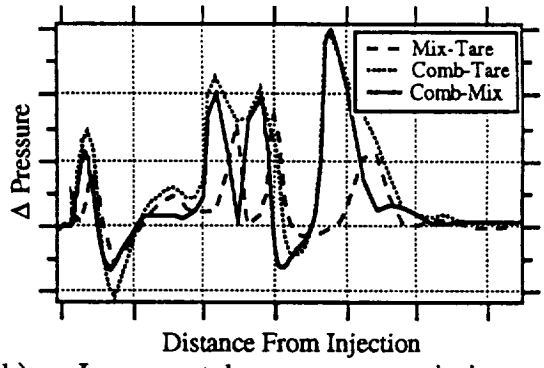

b) Incremental pressure variatio

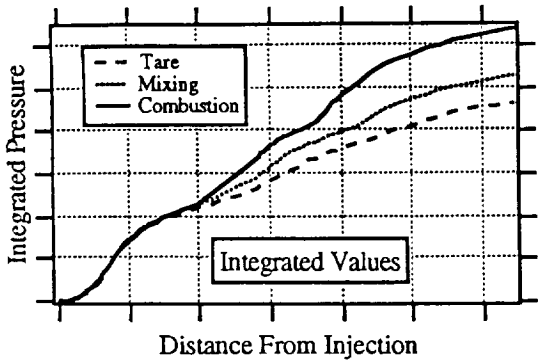

c) Integrated pressure variation

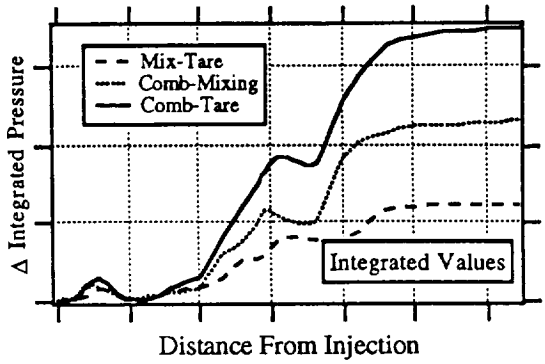

d) Integrated incremental pressure variation

Fig. 22. Computed combustor performance estimation

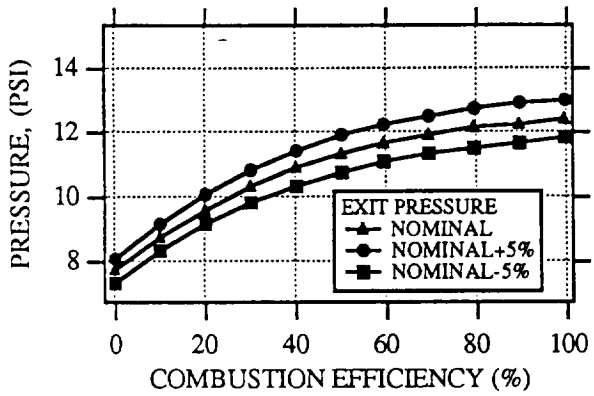

a) Sensitivity to pressure uncertainty

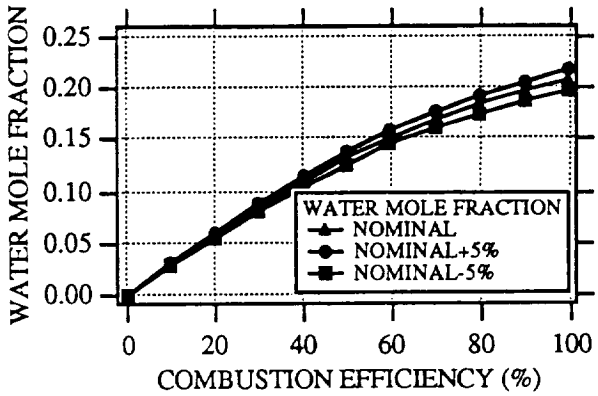

b Sensitivity to H_2O concentration uncertainty

Fig. 23 Combustion efficiency sensitivity

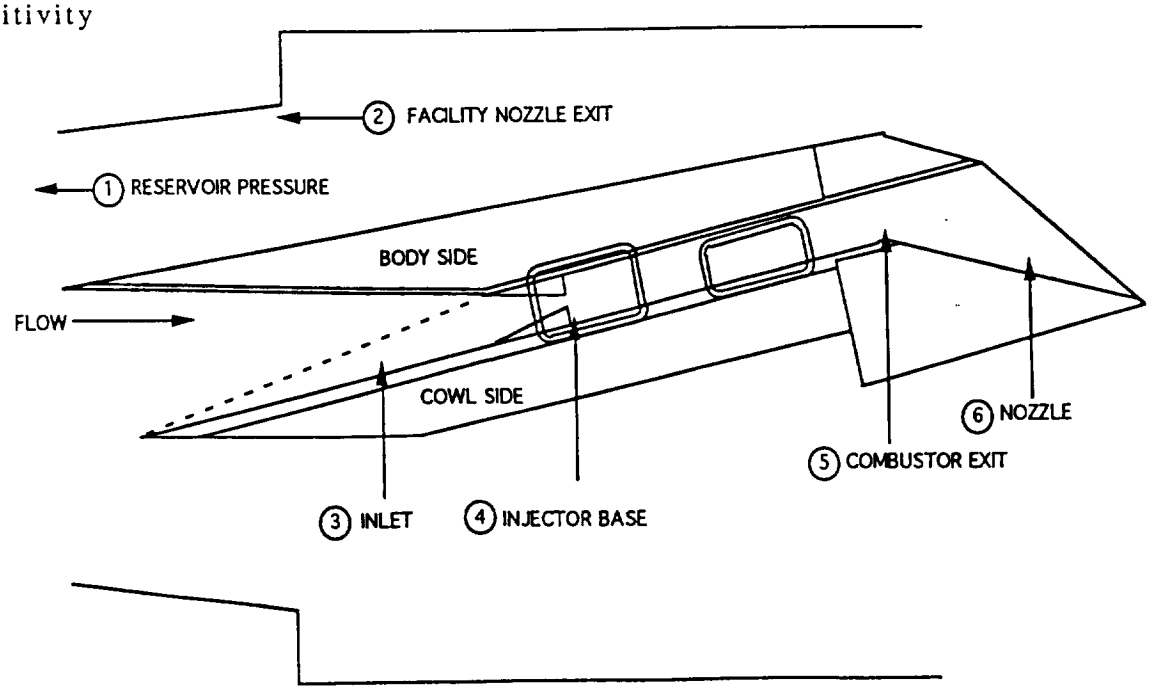

Fig. 24 Schematic of integrated combustor model and shock tunnel facility showing selected locations for pressure monitoring.

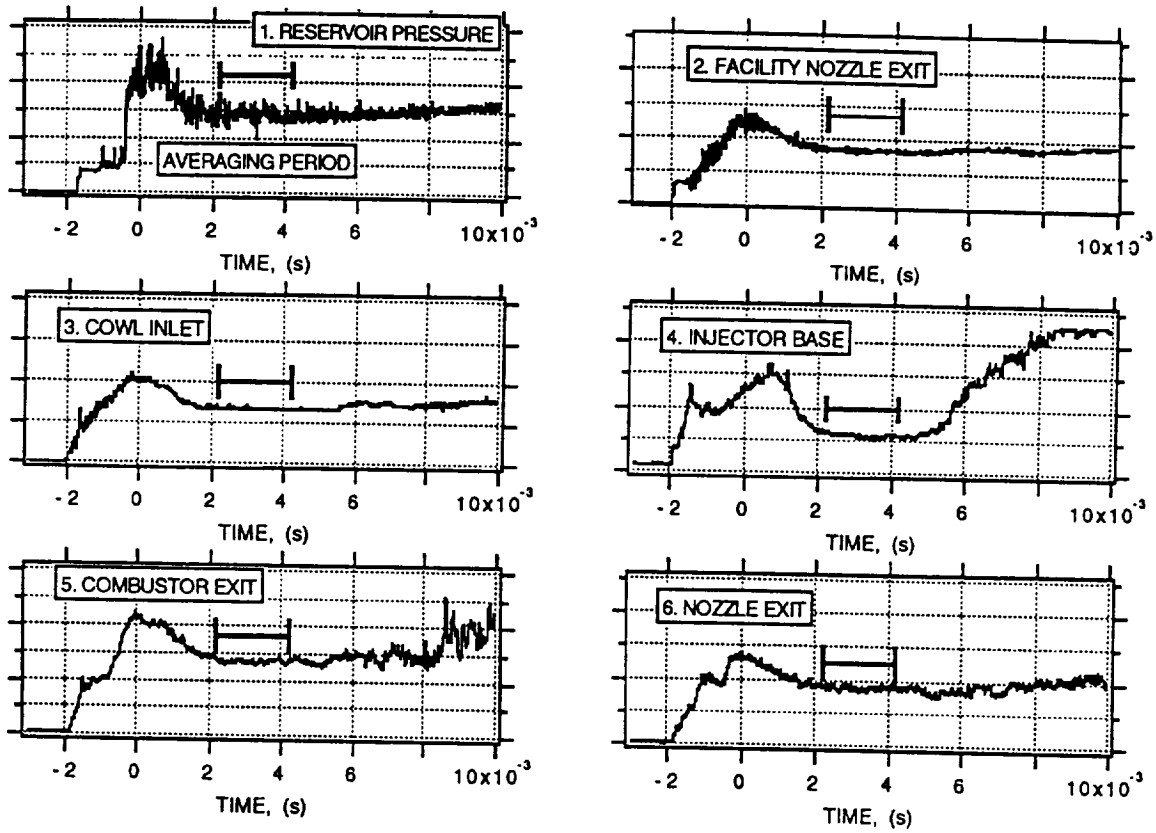

Fig. 25 Pressure vs. time traces for Mach 12 test

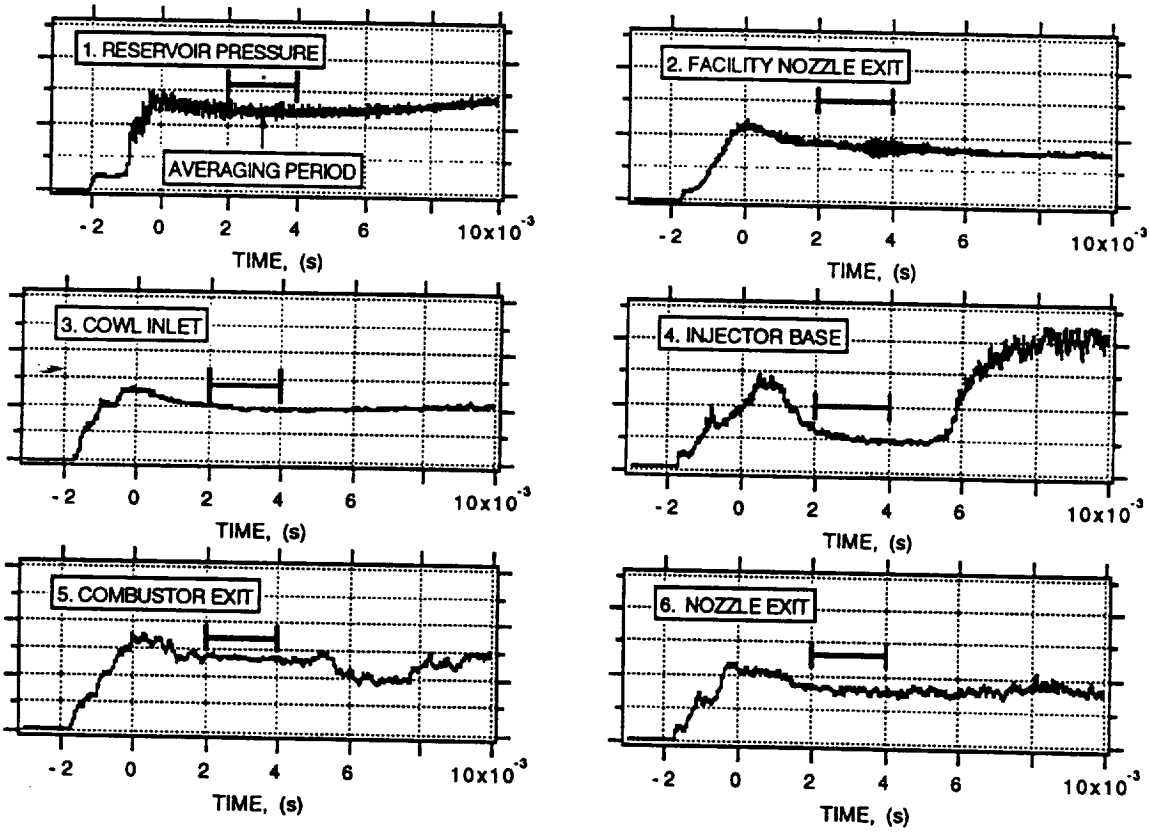

Fig. 26 Pressure vs. time traces for Mach 14 test

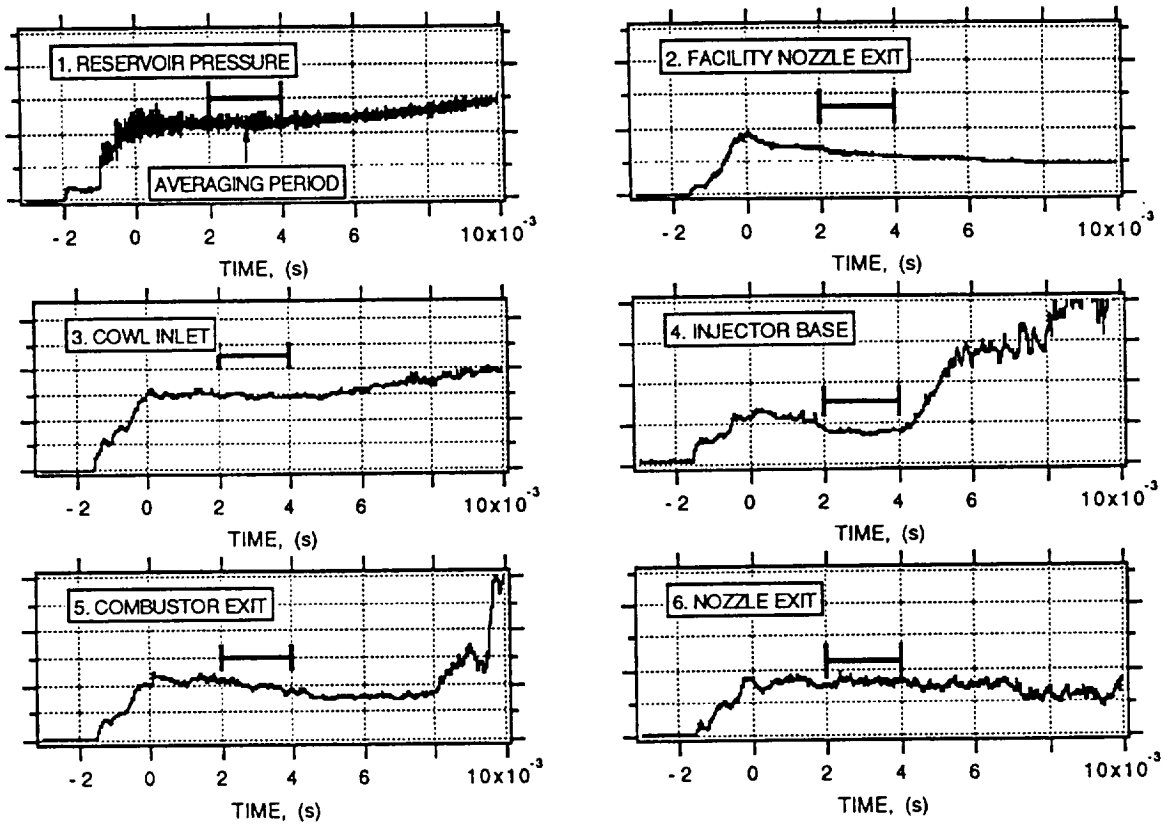

Fig. 27 Pressure vs. time traces for Mach 16 test

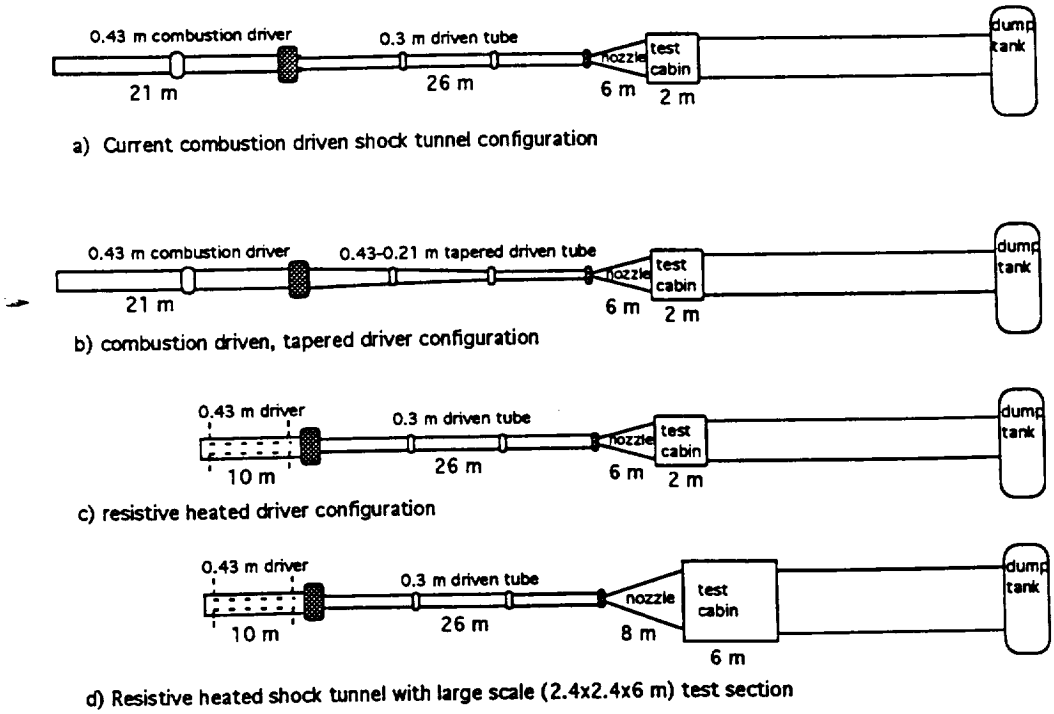

Fig. 28 Schematic of possible shock tunnel modifications

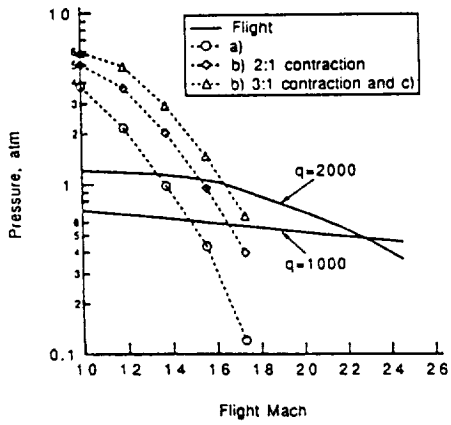

a) Combustor inlet static pressure

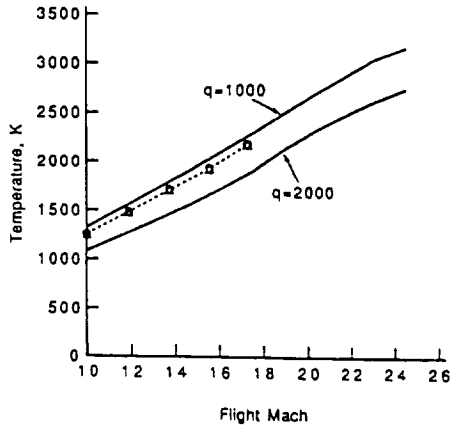

b) Combustor inlet static temperature

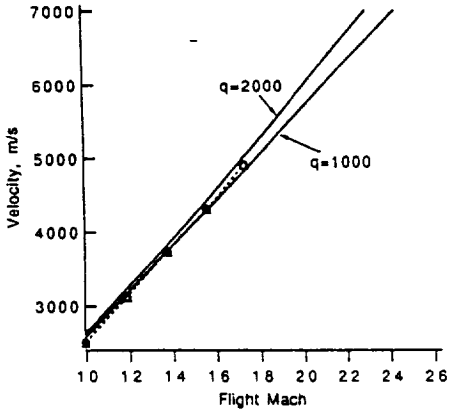

c) Combustor inlet velocity

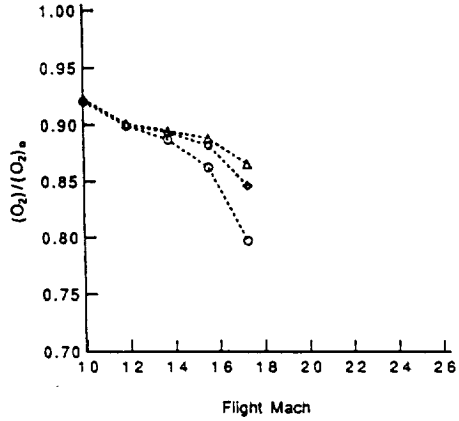

d) Combustor inlet oxygen concentration

Fig. 29. Combustor inlet simulation for enhanced pressure configurations

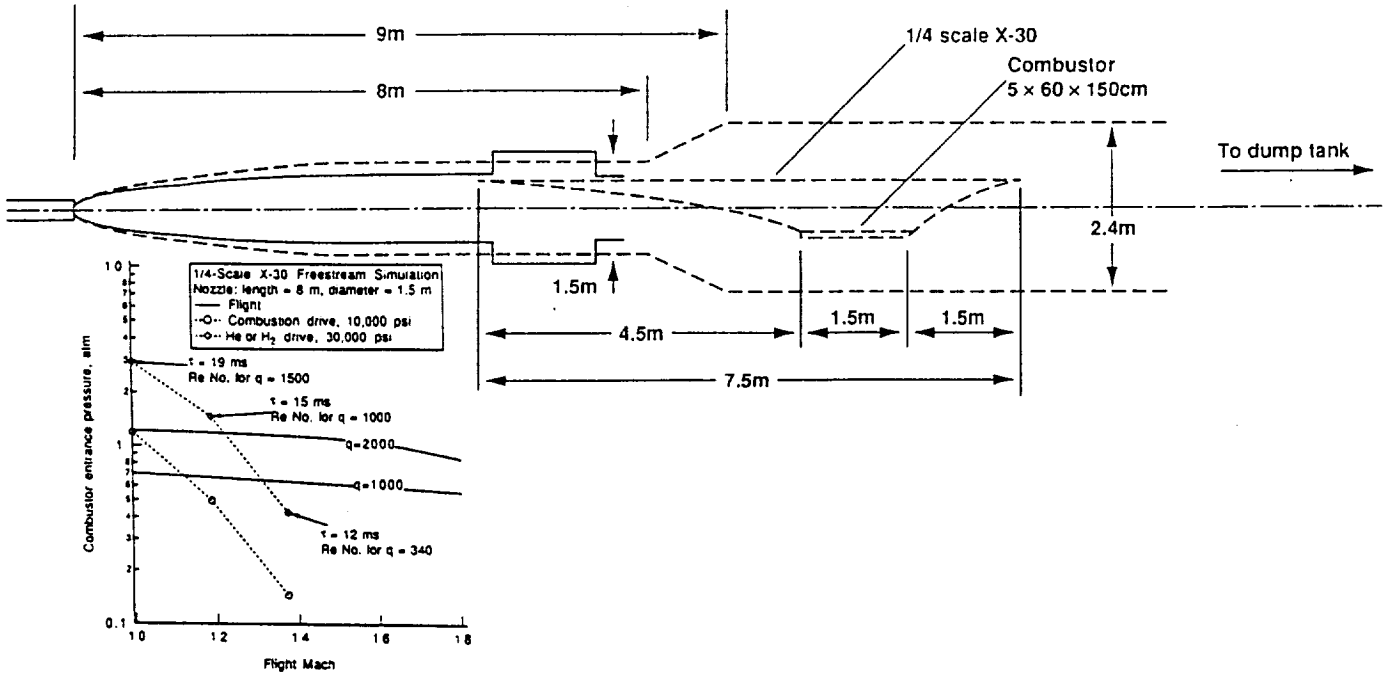

Fig.30. Increased facility scale and performance